

Global stability of SIR model with heterogeneous transmission rate modeled by the Preisach operator

Ruofei Guan, Jana Kopfová, Dmitrii Rachinskii

Abstract

In recent years, classical epidemic models, which assume stationary behavior of individuals, have been extended to include an adaptive heterogeneous response of the population to the current state of the epidemic. However, it is widely accepted that human behavior can exhibit history-dependence as a consequence of learned experiences. This history-dependence is similar to hysteresis effects that have been well-studied in control theory. To illustrate the importance of history-dependence for epidemic theory, we study dynamics of a variant of the SIRS model where individuals exhibit lazy-switch responses to prevalence dynamics. The resulting model, which includes the Preisach hysteresis operator, possesses a continuum of endemic equilibrium states characterized by different proportions of susceptible, infected and recovered populations. We discuss stability properties of the endemic equilibrium set and relate them to the degree of heterogeneity of the adaptive response. Our results support the argument that public health responses during the emergence of a new disease can have long-term consequences for subsequent management efforts. The main mathematical contribution of this work is a method of global stability analysis, which uses a family of Lyapunov functions corresponding to different branches of the hysteresis operator.

Keywords: SIR model, switching transmission rate, endemic equilibrium, connected set of equilibrium states, Preisach hysteresis operator, Lyapunov function

MSC: 34D23, 92D30, 92D25

1 Introduction

The standard SIR model assumes constant transmission rate (Kermack and McKendrick 1927). However, during epidemics, the transmission rate can change due to interventions of the health authorities and an adaptive response of the population to dynamics of the infectious disease. The role of the modulation of the transmission rate due to a human response to dynamics of epidemics has been widely studied (Capasso and Serio 1978; d’Onofrio and Manfredi 2009; d’Onofrio and Manfredi 2020). Preventive measures that decrease the transmission rate can include media campaigns raising awareness in the population about the current severity of the epidemic, massive vaccination campaigns, access to effective and affordable tests and medicines provided by the authorities, face covering in public places, quarantine and social distancing measures, transition to online teaching at schools and colleges, gathering and travel limitations, business restrictions and stay-at-home orders (Gostin and Wiley 2020; Marquioni and de Aguiar 2020; Center of Disease Control and Prevention 2021). Public participation in these measures can be partly mandatory and partly voluntary.

One major objective of preventive measures is flattening the curve, i.e. slowing down the spread of infection in order to keep the number of active disease cases at a manageable level dictated by the capacity of the health care system (Matrajt and Leung 2020). However, restrictive preventive measures can be typically introduced only for a limited period of time due to the economic and social cost they incur (Fairlie 2020). Because of these constraints, many prevention policies (such as the intervention protocols which have been recently implemented by the health authorities in order to contain the Covid-19 epidemic (Wilder-Smith et al. 2020) can be thought of, at least simplistically, as threshold based. As such, an intervention starts when a certain variable such as the number of daily new infections, the percentage of the occupied hospital beds or the effective reproduction number R reaches a critical threshold value set by the health or government authority (Department of Health and Human Services, Nebraska 2020; DeBenedetto and Ruiz 2021); the intervention is revoked when this variable drops below the level deemed safer. If the thresholds at which the intervention begins and ends are different, then *hysteresis* effect is present.

In their earliest form, hysteresis effects, which are commonly called a ‘backward bifurcation’ (a subcritical steady state bifurcation) in the epidemic theory literature, were clearly identified by Haderler and Chavez (1995) in their study of a core group. Hysteresis in adopting a ‘healthy behavior’ can also result from social contagion processes such as social interaction, reinforcement and imitation (Su et al. 2017; Wang et al. 2017). For instance, in the presence of imperfect vaccine, hysteresis loops of vaccination rate arise with respect to dynamic changes in the perceived cost of vaccination (Chen and Fu 2019) as individuals revisit their

vaccination decision in response to dynamics of the epidemic and through a social learning processes under peer influence. These hysteresis loops form a complex structure with minor loops nested within the maximal loop.

Hysteresis is a type of dependence of the state of a system on its past states (the term was first coined to describe magnetic hysteresis as lagging of the magnetization of a ferromagnetic material behind variations of the magnetizing field (Ewing 1881)). Characteristically, this lagging is determined by the past *values* of the phase variables and the *ordering* of the past events rather than the *timing* of those events. In particular, hysteresis is not associated with any explicit time scale and, as such, differs from the delayed response of systems with deviating argument (delayed and functional differential equations). In fact, hysteresis is defined as a *rate-independent* operator in (Visintin 1994) and is characterized by a durable effect of temporary stimuli in biological systems and population processes (Pimenov et al. 2012). Thus, the rate-independence of hysteresis and the prescribed time scale of systems with a deviating argument (and closely associated convolution operators) can be viewed as two idealizations which present a modeler with a choice of complementary mathematical tools for modeling a particular process.

The effectiveness of the prevention measures depends on the response of the population to the intervention policies and, in particular, the degree of homogeneity of this response. The ability and willingness of an individual to receive immunization or to follow community isolation policies depends on the level of trust to the authorities in the community, personal beliefs, perceived risk of contracting the disease, risk of possible complications and other factors, which vary with age, health condition, living circumstances, profession and social group (Guidry et al. 2021; Lazarus et al. 2021). All these variations contribute to the heterogeneity of the response of the society to the advent of an epidemic including behavioral changes. Effects of switching self-protecting behavior on the transmission of a disease were analyzed, for example, by Geoffard and Philipson (1996) and Chen (2004) who modeled a population of agents with heterogeneous preferences for taking protective actions using rational choice theory. Oscillatory vaccination dynamics in heterogeneous populations were identified by Reluga, Bauch and Galvani (2006). An important finding by Chen and Fu (2019) who studied a relaxation oscillator limit of these dynamics is that *hysteresis in adopting healthy behavior* becomes more pronounced with increasing heterogeneity of the population.

In this paper, we attempt to model the effect of *hysteresis* and *heterogeneity* in the response of the population to preventive measures on the epidemic trajectory. Our focus is on the global stability of the set of equilibrium states. We use a variant of the SIR model where the transmission rate depends on dynamics of the infected population. As a starting point, we adopt the approach used by Chladná et al. (2020) to modeling the homogeneous switched response of the population to the

varying number of infected individuals by a two-threshold two-state *relay operator*. In this model, it is assumed that the health authorities implement a two-threshold intervention policy whereby the intervention starts when the number of infected individuals exceeds a critical threshold value and stops whenever this number drops below a different (lower) threshold. The objective of the two-threshold policy is to navigate the system to the endemic equilibrium simultaneously keeping the number of infected individuals in check and not committing to continuous intervention. If the response is ideally homogeneous, then prevention measures are assumed to translate immediately to reduced values of the transmission coefficient and the effective reproduction number during the intervention. This response is characterized by the simplest rectangular hysteresis loop in the relationship between the density of the infected population and the transmission coefficient. The rectangular hysteresis loop can be considered as a model of the bi-stable response associated with the backward bifurcation.

Next, to reflect the heterogeneity of the response, the population is divided into multiple subpopulations, each characterized by a different pair of switching thresholds. In order to keep the model relatively simple, we apply averaging under additional simplifying assumptions as in Kopfová et al. (2021); Rouf and Rachinskii (2021). This leads to a differential model with just two variables, S and I , but with a complex operator relationship between the transmission rate and the density of the infected population I . As such, this operator relationship, known as the Preisach hysteresis operator (see, for example, Krasnosel'skii and Pokrovskii 1989; Mayergoyz 2003) accounts for hysteresis in the heterogeneous response. On the other hand, applications of differential models with a population of two-state relay operators to population dynamics date back to the pioneering work by Jäger and Hoppensteadt (1980).

We show that due to hysteresis, the heterogeneous model has a *connected continuum* of endemic equilibrium states characterized by different proportions of the susceptible, infected and recovered populations. We consider the convergence of the epidemic trajectory to this continuum. In mechanical systems, hysteresis incurs energy losses thus promoting convergence to an equilibrium state. This convergence can be shown using the energy potential as a Lyapunov function (for the construction of hysteretic thermodynamic potentials and examples, see Brokate and Sprekels (1996); Krejčí et al. (2013); Krejčí et al. (2019); related methods of the construction of the Lyapunov function for the problem of absolute stability of Lurie systems with hysteresis in the feedback loop can be found in Gelig and Yakubovich (1978) and the review Leonov et al.(2017). However, for SIR systems, hysteresis is a source of instability, which can lead to periodic oscillations corresponding to recurrent waves of infection (Chladná et al. 2020; Kopfová et al. 2021). The objective of this work is to show the convergence to the equilibrium

set if hysteresis has a limited magnitude (as quantified by an appropriate measure) and provide estimates for the magnitude of the hysteresis effect, which guarantee this stable scenario globally. A numerical case study of the dynamical scenarios exhibited by the heterogeneous SIR model considered below has been provided by Rachinskii and Rouf (2021).

To analyze stability, we interpret the SIR model with the Preisach operator as a switched system (di Bernardo et al. 2008) associated with an infinite family of nonlinear planar vector fields. Between the switching moments, a trajectory of the system is an integral curve of a particular globally stable vector field with the associated global Lyapunov function. The Preisach operator imposes non-trivial rules for switching from one vector field to another corresponding to switching from one to another branch of the hysteresis nonlinearity. We prove stability by carefully controlling (a) the increments of the Lyapunov functions along the trajectory between the switching points; and, (b) the difference of the Lyapunov functions corresponding to different vector fields (associated with different hysteresis branches) at the switching points. This methodology has been previously applied to a simpler special situation where the switching surface was the same for all the hysteresis branches (Kopfova et al. 2021 [27]). The main mathematical contribution of this paper is the extension of this method of global stability analysis to the more typical generic case when the switching surface changes dynamically depending on the history of the state.

The paper is organized as follows. In the next section, we discuss an SIR model with a hysteretic heterogeneous response. Stability results are presented in Section 3 and discussed in Section 4. The Appendix contains the proofs.

2 Model

2.1. The systems considered below adapt the standard dimensionless SIR model

$$\begin{aligned}\dot{I} &= \beta SI - (\gamma + \mu)I, \\ \dot{S} &= -\beta SI - \mu S + \mu\end{aligned}\tag{1}$$

with simple immigration demography, where I and S are the densities of the infected and susceptible populations, respectively; β is the transmission coefficient; γ is the recovery rate; and μ , is the departure rate due to the disease unrelated death and emigration. We assume a constant total population scaled to unity, hence the density of the recovered population $R = 1 - I - S$ can be removed from the system. The domain $I, S \geq 0, I + S \leq 1$ is positively invariant for system (1).

Re-scaling the time, one obtains the normalized system

$$\begin{aligned}\dot{I} &= R_0SI - I, \\ \dot{S} &= -R_0SI - \rho S + \rho,\end{aligned}\tag{2}$$

with the dimensionless parameters

$$R_0 = \frac{\beta}{\gamma + \mu}, \quad \rho = \frac{\mu}{\gamma + \mu} < 1.$$

Here R_0 is the *basic reproduction number* and $R = R_0S$ is the *effective reproduction number* for any given density S of the susceptible population. If $R_0 < 1$, then the *infection free equilibrium* $(I^*, S^*) = (0, 1)$ is globally stable in the closed positive quadrant. On the other hand, if $R_0 > 1$, then the infection free equilibrium is a saddle, and the positive *endemic equilibrium* (I_*, S_*) defined by

$$I_* = \left(1 - \frac{1}{R_0}\right)\rho, \quad S_* = \frac{1}{R_0}\tag{3}$$

is globally stable in the open positive quadrant. If

$$\rho(R_0)^2 < 4(R_0 - 1),\tag{4}$$

then the endemic equilibrium is of focus type.

2.2. A switched system with two flows of the form (1), which have different values of the basic reproduction number, $R_0 = R_0^{nat}$ and $R_0 = R_0^{int}$, was considered in Chladná et al., 2020; Rouf and Rachinskii, 2021. Following this work, we assume that the parameter ρ is the same for both flows and a switch from one flow to the other occurs when the density of the infected population reaches certain thresholds, $I = \alpha_1$ and $I = \alpha_2$, satisfying $0 < \alpha_1 < \alpha_2 < 1$. More precisely, it is postulated that the basic reproduction number instantaneously switches from the value R_0^{nat} to the value R_0^{int} when the variable $I = I(t)$ reaches the upper threshold value α_2 . On the other hand, R_0 switches back from the value R_0^{int} to the value R_0^{nat} as $I(t)$ reaches the lower threshold value α_1 , see Figure 1.

This two-threshold switching rule can be formalized using the standard *non-ideal relay operator*, which is also known as a rectangular hysteresis loop or a lazy switch (see e.g. Visintin 1994). The relay is characterized by the threshold parameters α_1, α_2 , and we use the notation $\alpha = (\alpha_1, \alpha_2)$. The function $I(t) : \mathbb{R}_+ \rightarrow \mathbb{R}$ is called the *input* of the relay. The *state* of the relay, denoted $r_\alpha(t)$, equals either 0 or 1 at any moment $t \in \mathbb{R}_+$. Specifically, given any continuous

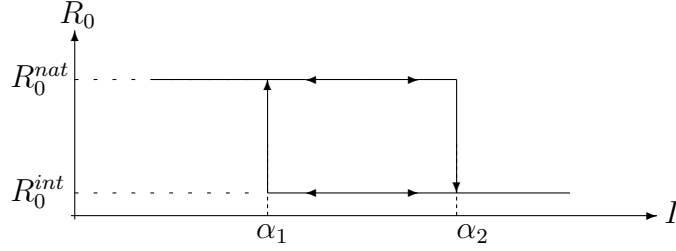


Figure 1: Switching rule (10) for the basic reproduction number. The vertical segments correspond to instantaneous transitions of the basic reproduction number from the value R_0^{nat} to R_0^{int} and back.

input $I(t) : \mathbb{R}_+ \rightarrow \mathbb{R}$ and an initial value of the state, $r_\alpha(0) = r_\alpha^0$, which satisfies the constraints

$$r_\alpha^0 \in \{0, 1\} \quad \text{if} \quad \alpha_1 < I(0) < \alpha_2; \quad (5)$$

$$r_\alpha^0 = 0 \quad \text{if} \quad I(0) \leq \alpha_1; \quad r_\alpha^0 = 1 \quad \text{if} \quad I(0) \geq \alpha_2, \quad (6)$$

the state of the relay at the future moments $t > 0$ is defined by the relations

$$r_\alpha(t) = \begin{cases} 0 & \text{if there is } t_1 \in [0, t] \text{ such that } I(t_1) \leq \alpha_1 \\ & \text{and } I(\tau) < \alpha_2 \text{ for all } \tau \in (t_1, t]; \\ 1 & \text{if there is } t_1 \in [0, t] \text{ such that } I(t_1) \geq \alpha_2 \\ & \text{and } I(\tau) > \alpha_1 \text{ for all } \tau \in (t_1, t]; \\ r_\alpha(0) & \text{if } \alpha_1 < I(\tau) < \alpha_2 \text{ for all } \tau \in [0, t]. \end{cases} \quad (7)$$

Function (7) will be denoted by

$$r_\alpha(t) = (\mathcal{R}_\alpha[r_\alpha^0]I)(t), \quad t \geq 0. \quad (8)$$

This standard short notation adopted from Brokate and Sprekels, 1996 stresses that the relay's state is dependent on the history of $I(t)$, i.e. (7) defines an operator which takes the function $I(t) : \mathbb{R}_+ \rightarrow \mathbb{R}$ rather than an instantaneous value of I as an input. Moreover, the function $r_\alpha(t) : \mathbb{R}_+ \rightarrow \{0, 1\}$ depends both on the input $I(t) : \mathbb{R}_+ \rightarrow \mathbb{R}$ and the initial state $r_\alpha(0) = r_\alpha^0$ of the relay. By definition (7) of the input-to-state map (8), the state satisfies the constraints

$$r_\alpha(t) = 1 \quad \text{whenever} \quad I(t) \geq \alpha_2; \quad r_\alpha(t) = 0 \quad \text{whenever} \quad I(t) \leq \alpha_1 \quad (9)$$

at all times. Further, the function (7) has at most a finite number of jumps between the values 0 and 1 on any finite time interval $t_0 \leq t \leq t_1$.

Using formula (7) and notation (8), the switching rule for the basic reproduction number depicted in Figure 1 can be expressed as

$$R_0(t) = R_0^{nat} - (R_0^{nat} - R_0^{int}) \cdot (\mathcal{R}_\alpha[r_\alpha^0]I)(t), \quad t \geq 0, \quad (10)$$

Combining equations (2) with formula (10) for $R_0 = R_0(t)$, one obtains a switched system. According to the interpretation discussed in the Introduction, the switched

system (2), (10) models the dynamics of the epidemic under the assumption that the health authorities implement the two-threshold intervention policy — an intervention begins when the density of infection (the number of active cases) exceeds the threshold value α_2 and is revoked when the density of infection drops below the lower threshold value α_1 . It is assumed that the intervention quickly translates into the reduction of the basic reproduction number; once the intervention stops, R_0 returns to the larger value.

As shown in Chladná et al. (2020); Rouf and Rachinskii (2021), each trajectory of switched system (2), (10) from the invariant domain $I, S \geq 0, I + S \leq 1$ converges to either an equilibrium state or a periodic orbit. In particular, depending on the positioning of the thresholds α_1, α_2 , the system can have either one attractor (an equilibrium state or a periodic orbit), or two attractors (two co-existing stable equilibrium states or a stable equilibrium state co-existing with a stable periodic orbit), or three attractors (two equilibrium states and one periodic orbit). For a periodic orbit with $I(t)$ oscillating between the values α_1 and α_2 , the point $(I(t), R_0(t))$ moves clockwise along the rectangular hysteresis loop shown in Figure 1.

2.3. Model (10) corresponds to an ideally homogeneous response of the population when all the individuals change their behavior simultaneously following the recommendation of the health authority. Now, we consider a model, in which several responses of the form (10), with different thresholds α , are combined because different groups of individuals respond differently to the advent and dynamics of an epidemic and to the interventions of the health authorities.

In particular, the ability and willingness to follow the recommendations of the health authority can vary significantly from one to another group of individuals for the same level of threat of contracting the disease. Multiple factors are at play such as the occupation, age, living environment and health conditions of an individual, to mention a few. In order to account for the heterogeneity of the individual response, let us divide the susceptible population into non-intersecting subpopulations S_α parameterized by points α of a subset $\Pi \subset \{\alpha = (\alpha_1, \alpha_2) : \alpha_1 < \alpha_2\}$ of the α -plane, assuming a homogeneous response within each group S_α . As a simplification, let us assume that the response of the infected population is homogeneous, i.e. all infected individuals act the same and don't change their behaviors over time, hence the heterogeneity of the transmission coefficient is due to the behavior of the susceptible individuals only. Further, assume that the basic reproduction number for the subpopulation S_α is given by (10) and the contact structure is separable. Then, the average basic reproduction number for the entire population at time t equals

$$R_0(t) = R_0^{nat} - (R_0^{nat} - R_0^{int}) \iint_{\Pi} (\mathcal{R}_\alpha[r_\alpha^0]I)(t) dF(\alpha), \quad t \in \mathbb{R}_+, \quad (11)$$

where the cumulative distribution function $F(\alpha)$ describes the distribution of the susceptible population S over the index set Π (the set of threshold pairs $\alpha = (\alpha_1, \alpha_2)$). The effective reproduction number at time t is then $R(t) = R_0(t)S(t)$. Finally, we assume for simplicity that the distribution function $F(\alpha)$ is independent of time, i.e. $F(\alpha)$ does not change with variations of I . In this case, the mapping of the space of continuous inputs $I(t) : \mathbb{R}_+ \rightarrow \mathbb{R}$ to the space of outputs $R_0(t) : \mathbb{R}_+ \rightarrow \mathbb{R}$ defined by (11) is known as the Preisach operator (see e.g. Krasnosel'skii and Pokrovskii 1989).

Under the above assumptions, the dynamics of the epidemic is modeled by system (2) where $R_0(t)$ is related to $I(t)$ by the Preisach operator (11), which accounts for the heterogeneity of the transmission coefficient among different subgroups of the susceptible population.

A similar system results from the assumption that the health authorities have multiple intervention policies (numbered $n = 1, \dots, N$) in place, each decreasing the transmission coefficient by a certain amount $\Delta\beta_n$ while the intervention is implemented (Rouf and Rachinskii 2021). The authorities aim to provide an adaptive response, which is adequate to the severity of the epidemic. Let us suppose that each intervention policy is guided by the two-threshold start/stop rule, such as in (10), associated with a particular pair of thresholds $\alpha^n = (\alpha_1^n, \alpha_2^n)$. The response of the population is assumed to be homogeneous. Under these assumptions, the basic reproduction number of system (2) is given by

$$R_0(t) = R_0^{nat} - \sum_{n=0}^{N-1} \hat{q}_n \cdot (\mathcal{R}_{\alpha^n}[r_{\alpha^n}^0]I)(t), \quad (12)$$

where $\hat{q}_n = \Delta\beta_n/(\gamma + \mu)$; hence, R_0 is set to change at multiple thresholds α_1^n, α_2^n . Operator (12), known as the discrete Preisach model, is a particular case of (11) with an atomic measure F .

Below we consider absolutely continuous distributions $F(\alpha)$ (see Appendix 5.1 for details). The corresponding operator (11), which is called the continuous Preisach model, can be written in the equivalent form

$$R_0(t) = R_0^{nat} - (R_0^{nat} - R_0^{int}) \iint_{\Pi} q(\alpha) (\mathcal{R}_{\alpha}[r_{\alpha}^0]I)(t) d\alpha_1 d\alpha_2, \quad t \geq 0, \quad (13)$$

where $0 < R_0^{int} < R_0^{nat}$ and $q = q(\alpha) : \Pi \rightarrow \mathbb{R}_+$ is a strictly positive measurable and bounded probability density function, i.e.

$$\iint_{\Pi} q(\alpha) d\alpha_1 d\alpha_2 = 1. \quad (14)$$

This operator can be approximated by discrete operators (12). We will assume that q is bounded. Also, in what follows,

$$\Pi = \{\alpha = (\alpha_1, \alpha_2) : 0 \leq \alpha_1 < \alpha_2 \leq 1\} \quad (15)$$

and

$$R_0^{nat} > R_0^{int} > 1. \quad (16)$$

The input-output diagram of the Preisach operator in Figure 2 illustrates the relation between $I(t)$ and $R_0(t)$ defined by equation (13). One can see that the point (I, R_0) switches from one *branch* $R_0(I)$ to another at every turning point of the input $I(t)$. The presence of multiple branches and hysteresis loops is a manifestation of the history-dependence, i.e. the output value $R_0(t)$ at a time t is determined not only by the concurrent value $I(t)$ of the input but also by some of the past input values $I(\tau)$ achieved on the time interval $\tau \in [0, t]$. Fundamental properties of the history-dependence, which are typical of hysteresis operators, are briefly discussed in Appendix 5.1.

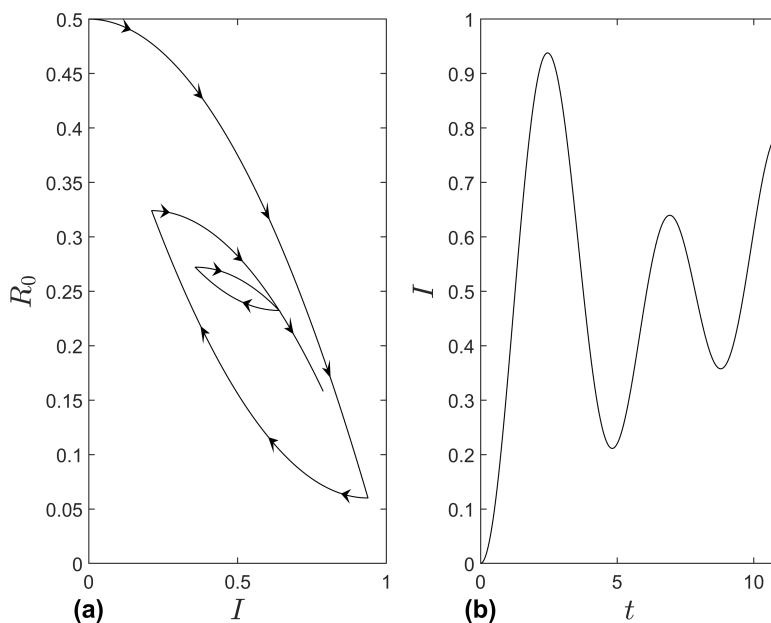


Figure 2: An example of the input-output diagram for the Preisach operator (13) on panel (a) for the input $I(t)$ shown on panel (b). The turning points on panel (a) correspond to local extrema of the input $I(t)$ on panel (b).

3 Results

3.1. Trajectories of system (2) coupled with the operator relationship (13) lie in the infinite-dimensional phase space \mathfrak{U} of triplets (I, S, r_α) , where the measurable function $r_\alpha = r(\alpha) : \Pi \rightarrow \{0, 1\}$ of the variable $\alpha = (\alpha_1, \alpha_2)$ describes the states

of the relays \mathcal{R}_α at a given moment (see Appendix 5.2 for details). Slightly abusing the notation, we will also refer to the two-dimensional curve $(I(t), S(t))$ as a trajectory, omitting the component (8) in the state space of the Preisach operator.

Let us first consider equilibrium states of system (2), (13). The components I , S , r_α of the solution and the basic reproduction number R_0 at an equilibrium state are constant, and R_0 is related to the function $r_\alpha = r(\alpha) : \Pi \rightarrow \{0, 1\}$ by the equation

$$R_0 = R_0^{nat} - (R_0^{nat} - R_0^{int}) \iint_{\Pi} q(\alpha) r_\alpha d\alpha_1 d\alpha_2. \quad (17)$$

Due to assumption (15) and the compatibility constraint (9), the inclusion $\alpha \in \Pi$ implies that all the relays are in state $r_\alpha = 0$ when $I = 0$. Therefore, system (2), (13) has a unique *infection free* equilibrium state

$$E^* = (I^*, S^*) = (0, 1), \quad (18)$$

in which the function $r_\alpha : \Pi \rightarrow \{0, 1\}$ is the identical zero and the basic reproduction number equals $R_0 = R_0^{nat}$ according to (17). On the other hand, it is easy to see that due to assumption (16), system (2), (13) also has a connected *continuum* of *endemic* equilibrium states

$$E_*^\theta = (I_*^\theta, S_*^\theta) = \left(\left(1 - \frac{1}{R_0^\theta}\right) \rho, \frac{1}{R_0^\theta} \right), \quad 0 \leq \theta \leq 1, \quad (19)$$

which are characterized by different proportions of the infected, susceptible and recovered populations and different values R_0^θ of the basic reproduction number (Rachinskii and Rouf 2021).

3.2. The phase space \mathfrak{U} of system (2), (13) is naturally embedded into the space $\mathbb{R}^2 \times L_1(\Pi; \mathbb{R})$ and is endowed with a metric by this embedding (see Appendix 5.2 for details). As such, local and global stability properties of trajectories of system (2), (13) are defined in the standard way. We consider the positively invariant set

$$\mathfrak{U}_0 = \{(I, S, r_\alpha) \in \mathfrak{U} : I > 0, S > 0, I + S \leq 1\}.$$

Theorem 1 *For any given $\rho > 0$, $R_0^{nat} > 1$ and a strictly positive probability density function $q = q(\alpha) : \Pi \rightarrow \mathbb{R}_+$ of the Preisach operator, there is an $\varepsilon \in (0, R_0^{nat} - 1)$ such that if $1 + \varepsilon \leq R_0^{int} < R_0^{nat}$, then the set of endemic equilibrium states of system (2), (13) is globally asymptotically stable in \mathfrak{U}_0 . Moreover, each trajectory from \mathfrak{U}_0 converges to an endemic equilibrium state. In particular, the components $I(t), S(t)$ of any trajectory from \mathfrak{U}_0 satisfy $(I(t), S(t)) \rightarrow E_*^\theta$ for some $\theta \in [0, 1]$.*

The proof presented in the Appendix provides an explicit estimate for the interval of values of $R_0^{int} \in [1 + \varepsilon, R_0^{nat})$, for which the set of endemic equilibrium states is globally stable. In particular, the global stability is guaranteed if the quantities ϵ_0 and κ defined by (27), (64) using (23), (62) are both positive.

4 Conclusion

We considered an SIR model where the transmission coefficient changes in response to dynamics of the epidemic. We aimed to emphasize that the adaptive response of the population to the state of the epidemic is typically heterogeneous and that this response can feature history-dependence in a form, which is similar to a hysteresis effect. Specifically, we adapted a two-state two-threshold hysteretic switch as a model of the adaptive response of an individual to the varying number of active cases. In an ideally homogeneous population, the two switching thresholds of the transmission coefficient can be imposed by the health authority which starts the intervention when the number of active cases exceeds a threshold α_1 and ends the intervention when the number of active cases drops below another threshold α_2 . In order to account for the possibility of a heterogeneous response among the susceptible individuals, we allowed a distribution of switching thresholds and modeled the aggregate response of the susceptible population by the Preisach operator. The variance of the distribution, σ^2 , measured the degree of heterogeneity of the public response to the interventions.

The resulting heterogeneous model is shown to have a continuum of endemic equilibrium states differing by the proportions of susceptible, infected and recovered populations. Numerical simulations of the model provided earlier by Rouf and Rachinskii, 2021 suggested that increasing the heterogeneity of the response by widening the spread of thresholds of different population groups (a larger variance σ^2) leads to a significant increase of the peak of infection during the epidemic. Moreover, a higher degree of heterogeneity of the public response also tends to steer the epidemic trajectory to an endemic equilibrium state with a higher prevalence and a lower proportion of the susceptible population. In other words, a more homogeneous response of the public to transmission prevention measures helps “flattening the curve” and can lead to lower prevalence and transmission rate when an endemic equilibrium state is reached after the epidemic. These results suggest that intervention programs are more effective when accompanied by education campaigns, which convey the importance of the intervention measures to the public thus ensuring a more homogeneous response from different population groups.

However, when the history-dependent two-threshold response in our model is ideally homogeneous, i.e. the transmission coefficient behaves as a lazy-switch, some threshold pairs lead to the convergence of the epidemic trajectory to a periodic orbit predicting recurrent outbreaks of the epidemic (Chladná et al. 2020). Emergence of sustained periodic oscillations of the prevalence was also shown numerically in a similar SIR model with vaccination when the heterogeneity of the response (measured by the variance σ^2 of the probability density function of the Preisach operator) decreases (Kopfová et al. 2021). This scenario is in line with

earlier findings by Reluga, Bauch and Galvani (2006) who identified stable oscillatory vaccination dynamics in heterogeneous populations and concluded that the more homogeneous the response of a population, the less likely vaccine uptake is to be stable. The stability theorem presented in this paper agrees with all these results suggesting that the heterogeneity of the adaptive response promotes the convergence of the epidemic trajectory to an equilibrium state. Indeed, the conditions of the theorem, which ensure the global stability of the endemic equilibrium set, require a sufficient degree of heterogeneity of the response. On the other hand, for a sufficiently homogeneous response, these conditions are violated leaving a possibility of undesirable non-equilibrium dynamics, i.e. a too homogeneous response can potentially trigger epidemic instability.

Thus, our results support the argument that a more homogeneous public response, which helps “flattening the curve” and tends to lead to a lower prevalence at the endemic state after the epidemic, comes at the price of a slower transitioning to the endemic state and a higher risk of epidemic instability. A higher degree of heterogeneity of the public response can stabilize and accelerate transitioning to an endemic state but after a higher infection peak; it also potentially results in a higher prevalence at the endemic equilibrium state after the epidemic.

The mathematical contribution of this paper is a method of global stability analysis, which uses a family of Lyapunov functions corresponding to different branches of the hysteresis operator. We applied this method for the first time to an epidemic model with an adaptive transmission rate. The method is potentially useful for analysis of other systems with hysteresis operators, which have a continuum of equilibrium states.

5 Appendix

5.1. Continuous Preisach model. Let us briefly recall a rigorous definition of the continuous Preisach operator (13) (Krasnosel’skii and Pokrovskii 1989). It involves a collection of non-ideal relays \mathcal{R}_α , which respond to the same continuous input $I(t) : \mathbb{R}_+ \rightarrow \mathbb{R}$ independently according to formula (7). The relays contributing to the system have different pairs of thresholds $\alpha = (\alpha_1, \alpha_2) \in \Pi$, where the subset Π of the half-plane $\{\alpha = (\alpha_1, \alpha_2) : \alpha_1 < \alpha_2\}$ is assumed to be measurable and bounded; the α -plane is called the Preisach plane. The output of the continuous Preisach model is the scalar-valued function $R_0(t) : \mathbb{R}_+ \rightarrow \mathbb{R}$ defined by (13), where $q(\alpha) : \Pi \rightarrow \mathbb{R}_+$ is a positive bounded measurable function (probability density function) representing the weights of the relays; and, r_α^0 is the initial state of the relay \mathcal{R}_α for any given $\alpha \in \Pi$. The function $r_\alpha^0 = r^0(\alpha) : \Pi \rightarrow \{0, 1\}$ of the variable $\alpha = (\alpha_1, \alpha_2)$ is referred to as the *initial state* function of the Preisach operator. It is assumed to be measurable and satisfy the constraints (5), (6), in

which case the initial state-input pair is called *compatible*. These requirements ensure that the integral in (13) is well-defined for each $t \geq 0$ and, furthermore, the output $R_0(t) : \mathbb{R}_+ \rightarrow \mathbb{R}$ of the Preisach model is a continuous function of time.

The function (7) with a fixed $t \geq 0$ and varying $\alpha \in \Pi$ is interpreted as the *state function* of the Preisach model at the moment t because it describes the states of all the relays at this moment; this state function $r_\alpha(t) = r(t; \alpha) : \Pi \rightarrow \{0, 1\}$ is an element of the space $L_1(\Pi; \mathbb{R})$ for each $t \geq 0$. In this sense, formula (7) defines the evolution of the state function in the space $L_1(\Pi; \mathbb{R})$ for a given input provided that the initial state-input pair is compatible. Moreover, the state function $r_\alpha(t) = r(t; \alpha) : \Pi \rightarrow \{0, 1\}$ and the concurrent input value $I(t)$ are compatible for each $t \geq 0$ and the *semigroup property* holds:

$$r_\alpha(\tau) = (\mathcal{R}_\alpha[r_\alpha^0]I)(\tau) \quad \Rightarrow \quad r_\alpha(t) = (\mathcal{R}_\alpha[r_\alpha(\tau)]I)(t) \quad \text{for any } \alpha \in \Pi, t \geq \tau \geq 0. \quad (20)$$

For brevity, let us denote the input-to-output operator of the Preisach model defined by (13) as

$$R_0(t) = (\mathcal{P}[r_\alpha^0]I)(t), \quad t \geq 0, \quad (21)$$

where both the input $I(t) : \mathbb{R}_+ \rightarrow \mathbb{R}$ and the initial state function $r_\alpha^0 = r^0(\alpha) : \Pi \rightarrow \{0, 1\}$ (which is compatible with the initial value of the input) are the arguments; the value of this operator is the output $R_0(t) : \mathbb{R}_+ \rightarrow \mathbb{R}$. An important property of the Preisach operator (13) is that it is Lipschitz continuous if $q(\alpha) : \Pi \rightarrow \mathbb{R}_+$ is bounded (Krasnosel'skii et al. 1989). More precisely, the relations

$$R_0^k(t) = (\mathcal{P}[r_\alpha^{0,k}]I^k)(t), \quad t \geq 0, \quad k = 1, 2,$$

and $0 \leq I^1(t), I^2(t) \leq 1$ ($t \geq 0$) imply

$$\|R_0^1(t) - R_0^2(t)\|_{C([0, \tau]; \mathbb{R})} \leq q_0 \left(\|r_\alpha^{0,1} - r_\alpha^{0,2}\|_{L_1(\Pi; \mathbb{R})} + \|I^1(t) - I^2(t)\|_{C([0, \tau]; \mathbb{R})} \right) \quad (22)$$

for any $\tau \geq 0$ with the Lipschitz constant

$$q_0 := (R_0^{nat} - R_0^{int}) \sup_{\alpha \in \Pi} q(\alpha). \quad (23)$$

5.2. Phase space of the system with the Preisach operator. Let \mathfrak{U} be the set of all triplets (I_0, S_0, r_α^0) , where $(I_0, S_0) \in \mathfrak{D} = \{(I, S) : 0 \leq I, S; I + S \leq 1\}$ and the state function $r_\alpha^0 = r^0(\alpha) : \Pi \rightarrow \{0, 1\}$ of the Preisach operator is compatible with I_0 . The set \mathfrak{U} is a natural phase space for system (2), (13). In particular, the global Lipschitz estimate (22) ensures (for example, using the Picard-Lindelöf type of argument) that for a given $(I_0, S_0, r_\alpha^0) \in \mathfrak{U}$, system (2), (13) has a unique local solution with the initial data $I(0) = I_0, S(0) = S_0$ and the initial state function r_α^0 of the Preisach operator (see e.g. the survey Leonov et al. 2017). This solution

satisfies $(I(t), S(t), r_\alpha(t)) \in \mathfrak{U}$ for each t in its domain. Further, the positive invariance of \mathfrak{D} implies that each solution is extendable to the whole semi-axis $t \in \mathbb{R}_+$. Due to the semigroup property (20), these solutions induce a continuous semi-flow in the phase space \mathfrak{U} , which is endowed with a metric by the natural embedding into the space $\mathbb{R}^2 \times L_1(\Pi; \mathbb{R})$. This construction leads to the standard definition of *local and global stability* including stability of equilibrium states and periodic solutions. In particular, an equilibrium is a triplet $(I_0, S_0, r_\alpha^0) \in \mathfrak{U}$ and a periodic solution is a periodic function $(I(t), S(t), r_\alpha(t)) : \mathbb{R}_+ \rightarrow \mathfrak{U}$ where the last component, viewed as a function $r_\alpha(t) = r(t; \alpha) : \mathbb{R}_+ \times \Pi \rightarrow \{0, 1\}$ of two variables $t \in \mathbb{R}_+$ and $\alpha \in \Pi$, is given by (8). The basic reproduction number (13) at an equilibrium is constant, while for a periodic solution the basic reproduction number $R_0(t)$ and the state function of the Preisach operator change periodically with the period of $I(t)$ and $S(t)$.

5.3. Switched system. A fundamental property of hysteresis operators, which is often used as their definition (see, e.g. Visintin 2006; Kluwer Encyclopedia of Mathematics 1997), is *rate-independence*. It means that for any increasing continuous function $\theta(t) : \mathbb{R}_+ \rightarrow \mathbb{R}_+$ (transformation of time) inputs $I(t)$ and $I(\theta(t))$ produce identical input-output diagrams such as in Figure ???. Due to the rate-independence property of the Preisach operator, given an initial state function $r^0 = r_\alpha^0 : \Pi \rightarrow \{0, 1\}$, there is a continuous function $R_{r^0} : \mathbb{R} \rightarrow \mathbb{R}$ such that every *monotone* input $I(t) : \mathbb{R}_+ \rightarrow \mathbb{R}$ (which is compatible with the state function at the initial moment) and the corresponding output (21) of the Preisach operator are related by

$$R_0(t) = R_{r^0}(I(t)), \quad t \geq 0.$$

The function $R_{r^0}(I)$ will be referred to as a *branch* of the Preisach operator. Hence, the state function $r^0 = r_\alpha^0$ parameterizes the infinite set of all possible branches. Due to the assumption that the density $q = q(\alpha)$ of the Preisach operator is positive, every branch $R_{r^0}(I)$ is a decreasing function on the interval $0 \leq I \leq 1$. Along with $R_{r^0}(I)$, the functions

$$f_{r^0}(I) = IR_{r^0}(I) \tag{24}$$

will play an important role.

With the above notation, if the first component $I(t)$ of a solution $(I(t), S(t), r(t)) : \mathbb{R}_+ \rightarrow \mathfrak{U}$ of system (2), (13) is monotone on a time interval $[t_k, t_{k+1}]$, then the pair $(I(t), S(t))$ is a solution of system

$$\begin{aligned} \dot{I} &= R(I)SI - I, \\ \dot{S} &= -R(I)SI - \rho S + \rho \end{aligned} \tag{25}$$

with

$$R(I) = R_{r^k}(I), \tag{26}$$

where $r^k = r(t_k)$, on the same time interval. This ordinary differential system will be called a branch of the operator-differential system (2), (13); again, the state function $r^k = r_\alpha^k$ of the Preisach operator parameterizes the set of ordinary differential systems (25), (26).

We see that dynamics of system (2), (13) can be interpreted as switched dynamics of planar systems (25), (26), where the switching moments are the turning points of the component I of a trajectory. As such, a switch occurs when a trajectory $(I(t), S(t))$ of system (25), (26) (with a fixed r^k) reaches the nullcline $\dot{I} = 0$, i.e. at the moment when $R_{r^k}(I(t))S(t) = 1$ (notice that the nullcline depends on r^k).

In what follows, the pair $(I(t), S(t))$ along with the triplet $(I(t), S(t), r(t)) : \mathbb{R}_+ \rightarrow \mathfrak{U}$ will be referred to as a solution of system (2), (13) whenever this doesn't cause confusion.

5.4. Proofs. Throughout the proofs we assume that $R_0^{nat} - R_0^{int} > 0$ is sufficiently small to ensure that the quantities ϵ_0, κ defined below by (27), (64) using (23), (62) satisfy $\epsilon_0, \kappa > 0$.

We first recall well-known stability properties of the planar ordinary differential system (25), which are ensured by the following lemmas.

Lemma 1 *If*

$$\epsilon_0 := R_0^{int} - q_0 > 0 \tag{27}$$

with q_0 given by (23), then for any branch $R(I)$ of the Preisach operator, the derivative of the function $f(I) = IR(I)$ satisfies

$$f'(I) \geq \epsilon_0.$$

Proof. From (22), it follows that $-q_0 \leq R'(I) \leq 0$. Combining this with $R(I) \geq R_0^{int}$ and $I \leq 1$, we obtain $f'(I) = R(I) + IR'(I) \geq \epsilon_0$. \square

Lemma 2 *System (25), where $R(I)$ is any branch of the Preisach operator, has a unique infection-free equilibrium $(I^*, S^*) = (0, 1)$ and a unique positive (endemic) equilibrium (I_*, S_*) , where I_* is a unique solution of*

$$\frac{1}{R(I)} = 1 - \frac{I}{\rho} \tag{28}$$

and $S_ = 1/R(I_*)$ (cf. (18), (19)). The infection-free equilibrium is unstable, while the positive equilibrium (I_*, S_*) is globally stable in the positive quadrant $I, S > 0$.*

Proof. By assumption, $1/R(0) = 1/R_{nat} < 1$ and $1/R(\rho) > 0$, hence equation (28) has a solution I_* in the interval $[0, \rho] \subset [0, 1]$. The measure density $q(\alpha)$

of the Preisach operator (13) is assumed to be positive, which implies that $R(I)$ is a decreasing function. Since the function $1/R(I)$ increases, while the function $1 - I/\rho$ decreases, this solution is unique.

The Jacobi matrix of system (25) at the infection-free equilibrium $(0, 1)$ has eigenvalues $\lambda_1 = R_{nat} - 1$, $\lambda_2 = -R_{nat} - \rho$, hence this equilibrium is a saddle due to the assumption $R_{nat} > 1$.

At the endemic equilibrium (I_*, S_*) , the characteristic polynomial of the Jacobi matrix of system (25) equals

$$P(\lambda) = \lambda^2 + \lambda(I_*R(I_*) + \rho - I_*R'(I_*)S_*) + I_*R(I_*) - \rho I_*R'(I_*)S_*.$$

Since $R(I)$ decreases, all coefficients of this polynomial are positive, hence all eigenvalues have negative real parts, and the endemic equilibrium is asymptotically stable.

We claim that

$$\begin{aligned} V(I, S) &= \int_{I_*}^I \left(1 - \frac{f(I_*)}{f(i)}\right) di + \int_{S_*}^S \left(1 - \frac{S_*}{s}\right) ds \\ &= I - I_* + S - S_* - f(I_*) \int_{I_*}^I \frac{di}{f(i)} - S_* \ln \frac{S}{S_*}. \end{aligned} \quad (29)$$

is a Lyapunov function for system (25) in the positive quadrant.

Indeed, $V(I_*, S_*) = 0$, and Lemma 1 implies that $V(I, S) > 0$ for $I, S > 0$ except at the point (I_*, S_*) . Further, $V \rightarrow \infty$ if either $I + S \rightarrow \infty$ or $S \rightarrow 0$ or $I \rightarrow 0$ (the latter follows from $f(0) = 0$). On the other hand, using the notation

$$R_* = R(I_*), \quad f_* = f(I_*) = I_*R(I_*)$$

and $R = R(I)$, $f = f(I)$, the time derivative of V along a trajectory of system (25) equals

$$\begin{aligned} \dot{V} &= \left(1 - \frac{S_*}{S}\right) \rho(1 - S) - I + S_*f + \frac{f_*I}{f} - Sf_* \\ &= \frac{\rho}{S}(S - S_*)(1 - S) - f_*(S - S_*) + S_*(f - f_*) - I \left(1 - \frac{f_*}{f}\right) \\ &= \frac{\rho}{S}(S - S_*)(1 - S) - (S - S_*) \frac{\rho(1 - S_*)}{S_*} + (S_*f - I) \left(1 - \frac{f_*}{f}\right), \end{aligned}$$

where we used that $I_* = \rho(1 - S_*) = \rho(1 - I_*/f_*)$ due to Lemma 2. Equivalently,

$$\begin{aligned} \dot{V} &= \rho(S - S_*) \left(\frac{1}{S} - \frac{1}{S_*}\right) + \left(\frac{I_*f}{f_*} - I\right) \left(1 - \frac{f_*}{f}\right) \\ &= -\frac{\rho}{SS_*}(S - S_*)^2 + \frac{I_*}{f}(f - f_*) \cdot \frac{I}{f_*} \left(\frac{f}{I} - \frac{f_*}{I_*}\right) \\ &= -\frac{\rho}{SS_*}(S - S_*)^2 + \frac{1}{RR_*}(f - f_*)(R - R_*). \end{aligned}$$

Since the function $R = R(I)$ decreases and the function $f = f(I)$ increases (Lemma 1), we conclude that

$$\dot{V} \leq -\frac{\rho}{SS_*}(S - S_*)^2 < 0, \quad (I, S) \neq (I_*, S_*). \quad (30)$$

Hence, the equilibrium (I_*, S_*) is globally stable in the positive quadrant. \square

It turns out that the function V is convex.

Lemma 3 *All the level sets $\{(I, S) : V(I, S) < c\}$, $c > 0$, of the function V are convex.*

Proof. Denoting the partial derivatives of the function V by V_I, V_S , the curvature of the level line $\{(I, S) : V(I, S) = c\}$ of V for any $c > 0$ is given by

$$\kappa = -\frac{V_{SS}(V_I)^2 + V_{II}(V_S)^2 - 2V_{IS}V_IV_S}{(V_S^2 + V_I^2)^{3/2}} = -\frac{V_{SS}(V_I)^2 + V_{II}(V_S)^2}{(V_S^2 + V_I^2)^{3/2}},$$

because $V_{IS} = 0$. Using that

$$V_I = 1 - \frac{f(I_*)}{f(I)}, \quad V_S = 1 - \frac{S_*}{S}, \quad V_{II} = \frac{f'(I)f(I_*)}{f^2(I)}, \quad V_{SS} = \frac{S_*}{S^2}$$

and that $f'(I) > 0$ due to Lemma 1, we obtain $\kappa < 0$, which completes the proof. \square

Let us consider the trajectory $(I(\cdot), S(\cdot), r(\cdot)) : \mathbb{R}_+ \rightarrow \mathfrak{U}$ of system (2), (13) and the corresponding planar curve $(I(\cdot), S(\cdot)) : \mathbb{R}_+ \rightarrow \mathbb{R}^2$. Consider the sequence $\mathbb{T} = \{t_k\}$ of successive switching moments $0 = t_0 < t_1 < t_2 < \dots$ such that

- The restriction of $(I(\cdot), S(\cdot)) : \mathbb{R}_+ \rightarrow \mathbb{R}^2$ to each interval (t_k, t_{k+1}) , $t_k, t_{k+1} \in \mathbb{T}$ is a solution of system (25) with $R(I) = R_{r(t_k)}(I)$ satisfying

$$R_{r(t_k)}(I(t))S(t) \neq 1, \quad t \in (t_k, t_{k+1}); \quad R(I(t_{k+1}))S(t_{k+1}) = 1. \quad (31)$$

- In addition, if the set $\mathbb{T} = \{t_0, \dots, t_N\}$ is finite, then the restriction of $(I(\cdot), S(\cdot)) : \mathbb{R}_+ \rightarrow \mathbb{R}^2$ to the infinite interval (t_N, ∞) is a solution of system (25) with $R(I) = R_{r(t_N)}(I)$ satisfying

$$R_{r(t_N)}(I(t))S(t) \neq 1, \quad t > t_N.$$

If the set \mathbb{T} is finite, the trajectory of system (2), (13) follows the flow (25), (26) on the interval $[t_N, \infty)$ and due to Lemma 2 converges to an equilibrium. In this scenario, this equilibrium of (25), (26) is a node.

We continue the proof assuming that $\mathbb{T} = \{t_k\}$ is infinite, i.e. there is an infinite sequence of switches along the trajectory. Let

$$I_k = I(t_k), \quad S_k = S(t_k).$$

Denote by $V_k(I, S)$ the Lyapunov function (36) for system (25), (26) (where $r^k = r(t_k)$) and by (I_*^k, S_*^k) the positive (endemic) equilibrium of this system. We will also use the notation $R_k(I) = R_{r(t_k)}(I)$. The next lemma provides an estimate for the (negative) increment

$$\Delta V_k := V_k(I_{k+1}, S_{k+1}) - V_k(I_k, S_k) \quad (32)$$

of this function along the trajectory on the time interval $[t_k, t_{k+1}]$.

Lemma 4 *If $R_{r(t_k)}(I(t))S(t) > 1$ on (t_k, t_{k+1}) (cf. (31)), then the increment (32) of the Lyapunov function V_k along the trajectory satisfies*

$$\Delta V_k \leq -\frac{\rho}{4}(I_{k+1} - I_*^k) \sqrt{S_M \int_{I_*^k}^{I_{k+1}} \left(1 - \frac{f(I_*^k)}{f(i)}\right) di}, \quad (33)$$

where $M = (I_M, S_M)$ is the highest point of the level line $V_k(I, S) = V_k(I_{k+1}, S_{k+1})$ of the Lyapunov function V_k , see Figure 3.

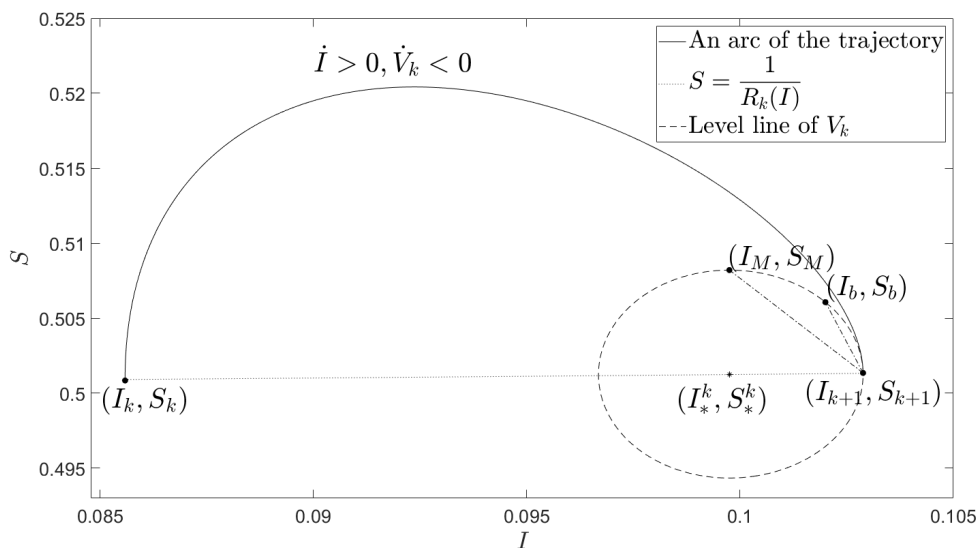


Figure 3: An arc of a trajectory of system (2), (13) satisfying $R_k(I(t))S(t) \geq 1$.

Proof. At the point $M = (I_M, S_M)$,

$$0 = \left. \frac{\partial V_k}{\partial I} \right|_M = 1 - \frac{f(I_*^k)}{f(I_M)},$$

which is equivalent to $f(I_*^k) = f(I_M)$. Since $f(I)$ increases, it follows that $I_M = I_*^k$, hence $M = (I_*^k, S_M)$ and

$$V_k(I_*^k, S_M) = S_M - S_*^k - S_*^k \ln \frac{S_M}{S_*^k}.$$

Consider a point (I_b, S_b) on the arc of the level line of V_k connecting the points M and (I_{k+1}, S_{k+1}) . Due to Lemma 3,

$$\frac{S_b - S_{k+1}}{I_{k+1} - I_b} \geq \frac{S_M - S_{k+1}}{I_{k+1} - I_*^k}$$

(see Figure 3). Equivalently,

$$I_{k+1} - I_b \leq \frac{S_b - S_{k+1}}{S_M - S_{k+1}} (I_{k+1} - I_*^k).$$

This implies the estimate

$$I_b - I_*^k \geq I_{k+1} - I_*^k - \frac{S_b - S_{k+1}}{S_M - S_{k+1}} (I_{k+1} - I_*^k) = \frac{S_M - S_b}{S_M - S_{k+1}} (I_{k+1} - I_*^k). \quad (34)$$

In the domain $I \geq I_*^k, S \geq 1/R_k(I)$, we have $1/R_k(I) \geq 1/R_k(I_*^k) = S_*^k$, which implies $0 \leq S - 1/R_k(I) \leq S - S_*^k$. Hence, relation (30) implies that along the trajectory,

$$\begin{aligned} \frac{dV_k}{dI} = \frac{\dot{V}_k}{\dot{I}} &\leq -\frac{\rho}{SS_*^k IR_k(I)} \cdot \frac{(S - S_*^k)^2}{(S - 1/R_k(I))} \leq -\frac{\rho}{SS_*^k IR_k(I_*^k)} (S - S_*^k) \\ &= -\frac{\rho}{SI} (S - S_*^k) \leq -\frac{\rho}{I} (S - S_*^k). \end{aligned}$$

Since V_k decreases along the trajectory, the segment of the trajectory with $t \in (t_k, t_{k+1})$ lies above the level line of V_k , hence for this segment $I \in [I_*^k, I_b]$ implies $S \geq S_b$ and

$$\frac{dV_k}{dI} \leq -\frac{\rho}{I} (S_b - S_*^k). \quad (35)$$

The relation $\dot{I}(t) > 0$, $t \in (t_k, t_{k+1})$, implies that the arc of the trajectory for this time interval admits a parameterization $(I, \hat{S}(I))$, $I \in [I_k, I_{k+1}]$. Therefore, integrating (35) over the interval $[I_*^k, I_b]$, we obtain

$$V_k(I_b, \hat{S}(I_b)) - V_k(I_*^k, \hat{S}(I_*^k)) \leq -\rho(S_b - S_*^k) \ln \frac{I_b}{I_*^k}.$$

Further, using the identity $\ln(1+x) \geq x/(1+x)$, $x \geq -1$, we arrive at

$$V_k(I_b, \hat{S}(I_b)) - V_k(I_*^k, \hat{S}(I_*^k)) \leq -\rho(S_b - S_*^k) \frac{I_b - I_*^k}{I_b} \leq -\rho(S_b - S_*^k)(I_b - I_*^k)$$

and due to (34),

$$V_k(I_b, \hat{S}(I_b)) - V_k(I_*^k, \hat{S}(I_*^k)) \leq -\rho \frac{(S_b - S_*^k)(S_M - S_b)(I_{k+1} - I_*^k)}{S_M - S_{k+1}}. \quad (36)$$

The maximum of the function $\frac{(S_b - S_*^k)(S_M - S_b)}{S_M - S_{k+1}}$ on the interval $[S_{k+1}, S_M]$ is achieved at $S_{k+1} = (S_M + S_*^k)/2$, hence

$$\max_{S_b \in [S_{k+1}, S_M]} \frac{(S_b - S_*^k)(S_M - S_b)}{S_M - S_{k+1}} \geq \frac{(S_M - S_*^k)^2}{4(S_M - S_{k+1})} \geq \frac{(S_M - S_*^k)^2}{4(S_M - S_*^k)} = \frac{S_M - S_*^k}{4}.$$

Therefore, from (36) it follows that

$$V_k(I_b, \hat{S}(I_b)) - V_k(I_*^k, \hat{S}(I_*^k)) \leq -\frac{\rho}{4}(I_{k+1} - I_*^k)(S_M - S_*^k).$$

Since V_k decreases along the trajectory, this estimate implies

$$\Delta V_k \leq -\frac{\rho}{4}(I_{k+1} - I_*^k)(S_M - S_*^k). \quad (37)$$

Finally, let us estimate $S_M - S_*^k$. Since V_k has the same value at the points (I_*^k, S_M) and (I_{k+1}, S_{k+1}) , we have

$$S_M - S_*^k - S_*^k \ln \frac{S_M}{S_*^k} = I_{k+1} - I_*^k - f(I_*^k) \int_{I_*^k}^{I_{k+1}} \frac{di}{f(i)} + S_{k+1} - S_*^k - S_*^k \ln \frac{S_{k+1}}{S_*^k},$$

which implies

$$S_M - S_{k+1} - S_*^k \ln \frac{S_M}{S_{k+1}} = \int_{I_*^k}^{I_{k+1}} \left(1 - \frac{f(I_*^k)}{f(i)}\right) di.$$

We estimate the left hand side of this equation using $\ln(1+x) \geq x/(1+x)$, $x \geq -1$:

$$S_M - S_{k+1} - S_*^k \ln \frac{S_M}{S_{k+1}} \leq S_M - S_{k+1} - \frac{S_*^k(S_M - S_{k+1})}{S_M} = \left(1 - \frac{S_*^k}{S_M}\right)(S_M - S_{k+1}),$$

hence

$$\frac{1}{S_M}(S_M - S_*^k)(S_M - S_{k+1}) \geq \int_{I_*^k}^{I_{k+1}} \left(1 - \frac{f(I_*^k)}{f(i)}\right) di.$$

Since $S_*^k < S_{k+1}$, this implies

$$(S_M - S_*^k)^2 \geq S_M \int_{I_*^k}^{I_{k+1}} \left(1 - \frac{f(I_*^k)}{f(i)}\right) di. \quad (38)$$

Combining this relation with (37), we obtain (33). \square

Next, we estimate the difference

$$\tilde{\Delta}V_k := V_{k+1}(I_{k+1}, S_{k+1}) - V_k(I_{k+1}, S_{k+1}) \quad (39)$$

between the values of Lyapunov functions V_{k+1} and V_k at the point (I_{k+1}, S_{k+1}) . We begin with the following statement.

Lemma 5 *Under the assumptions of Lemma 4,*

$$0 \leq I_*^k - I_*^{k+1} = \rho(S_*^{k+1} - S_*^k) \leq \frac{\rho q_0}{R_{k+1}(I_*^{k+1})R_k(I_*^k)} (I_{k+1} - I_*^k). \quad (40)$$

Proof. Consider the branch $R_k(I) := R_{r(t_k)}(I)$ of the Preisach operator (see Section 5.3), the corresponding function $f_k(I) := IR_k(I)$ and the endemic equilibrium (I_*^k, S_*^k) of system (25), (26) for this branch:

$$S_*^k = 1 - \frac{I_*^k}{\rho} = \frac{1}{R_k(I_*^k)}.$$

These equations imply

$$S_*^{k+1} - S_*^k = \frac{1}{\rho}(I_*^k - I_*^{k+1})$$

and

$$\begin{aligned} \frac{I_*^k - I_*^{k+1}}{\rho} &= \frac{1}{R_{k+1}(I_*^{k+1})} - \frac{1}{R_k(I_*^k)} = \frac{R_k(I_*^k) - R_{k+1}(I_*^k) + R_{k+1}(I_*^k) - R_{k+1}(I_*^{k+1})}{R_{k+1}(I_*^{k+1})R_k(I_*^k)} \\ &= \frac{1}{R_{k+1}(I_*^{k+1})R_k(I_*^k)} (R_k(I_*^k) - R_{k+1}(I_*^k) + R'_{k+1}(\hat{I})(I_*^k - I_*^{k+1})) \end{aligned}$$

for an intermediate value of \hat{I} between I_*^k and I_*^{k+1} .

If we assume that $I_*^{k+1} > I_*^k$, then we arrive at a contradiction:

$$0 > \frac{1}{\rho}(I_*^k - I_*^{k+1}) = \frac{1}{R_{k+1}(I_*^{k+1})R_k(I_*^k)} (R_k(I_*^k) - R_{k+1}(I_*^k) + R'_{k+1}(\hat{I})(I_*^k - I_*^{k+1})) \geq 0$$

because $R_{k+1}(I)$ decreases and (22) implies that

$$0 \leq R_k(I_*^k) - R_{k+1}(I_*^k) \leq q_0(I_{k+1} - I_*^k). \quad (41)$$

Hence, $I_*^{k+1} \leq I_*^k$, and consequently $S_*^{k+1} \geq S_*^k$ as well as

$$0 \leq S_*^{k+1} - S_*^k = \frac{1}{\rho}(I_*^k - I_*^{k+1}) \leq \frac{R_k(I_*^k) - R_{k+1}(I_*^k)}{R_{k+1}(I_*^{k+1})R_k(I_*^k)}. \quad (42)$$

Combining (41) and (42), we obtain (40). \square

We use Lemma 5 to prove the following estimate for the difference (39).

Lemma 6 *Under the assumptions of Lemma 4, the difference (39) satisfies*

$$\tilde{\Delta}V_k \leq \frac{q_0(I_{k+1} - I_*^k)^2}{R_k(I_*^k)} \left(\frac{\rho^2 q_0}{R_{k+1}^2(I_*^{k+1})f_k(I_*^k)} + \frac{\rho}{f_k(I_*^k)} + 1 \right). \quad (43)$$

Proof. By the definition of the Lyapunov function, $\tilde{\Delta}V_k = \Delta_S + \Delta_I$, where

$$\begin{aligned} \Delta_S &= \int_{S_*^{k+1}}^{S_{k+1}} \left(1 - \frac{S_*^{k+1}}{s}\right) ds - \int_{S_*^k}^{S_{k+1}} \left(1 - \frac{S_*^k}{s}\right) ds \\ &= - \int_{S_*^k}^{S_*^{k+1}} \left(1 - \frac{S_*^k}{s}\right) ds - \int_{S_*^{k+1}}^{S_{k+1}} \left(\frac{S_*^{k+1} - S_*^k}{s}\right) ds, \\ \Delta_I &= \int_{I_*^{k+1}}^{I_{k+1}} \left(1 - \frac{f_{k+1}(I_*^{k+1})}{f_{k+1}(i)}\right) di - \int_{I_*^k}^{I_{k+1}} \left(1 - \frac{f_k(I_*^k)}{f_k(i)}\right) di \\ &= - \int_{I_*^k}^{I_{k+1}} \left(\frac{f_{k+1}(I_*^{k+1})}{f_{k+1}(i)} - \frac{f_k(I_*^k)}{f_k(i)}\right) di - \int_{I_*^k}^{I_*^{k+1}} \left(1 - \frac{f_{k+1}(I_*^{k+1})}{f_{k+1}(i)}\right) di \\ &= - \int_{I_*^k}^{I_{k+1}} \left(\frac{f_{k+1}(I_*^{k+1})}{f_{k+1}(i)} - \frac{f_{k+1}(I_*^{k+1})}{f_k(i)}\right) di - \int_{I_*^k}^{I_{k+1}} \frac{f_{k+1}(I_*^{k+1}) - f_k(I_*^k)}{f_k(i)} di \\ &\quad - \int_{I_*^k}^{I_*^{k+1}} \left(1 - \frac{f_{k+1}(I_*^{k+1})}{f_{k+1}(i)}\right) di. \end{aligned}$$

By Lemma 5, $S_*^k \leq S_*^{k+1} \leq S_{k+1}$, hence

$$\int_{S_*^k}^{S_*^{k+1}} \left(1 - \frac{S_*^k}{s}\right) ds \geq 0, \quad \int_{S_*^{k+1}}^{S_{k+1}} \left(\frac{S_*^{k+1} - S_*^k}{s}\right) ds \geq 0, \quad (44)$$

and consequently $\Delta_S \leq 0$. Also, the relation $R_{k+1}(I) \leq R_k(I)$, $I \leq I_{k+1}$, implies that

$$\int_{I_*^k}^{I_{k+1}} \left(\frac{f_{k+1}(I_*^{k+1})}{f_{k+1}(i)} - \frac{f_{k+1}(I_*^{k+1})}{f_k(i)}\right) di = \int_{I_*^k}^{I_{k+1}} \frac{f_{k+1}(I_*^{k+1})}{i} \left(\frac{1}{R_{k+1}(i)} - \frac{1}{R_k(i)}\right) di \geq 0, \quad (45)$$

therefore

$$\tilde{\Delta}V_k \leq \Delta_I \leq - \int_{I_*^k}^{I_*^{k+1}} \left(1 - \frac{f_{k+1}(I_*^{k+1})}{f_{k+1}(i)} \right) di - \int_{I_*^k}^{I_*^{k+1}} \frac{f_{k+1}(I_*^{k+1}) - f_k(I_*^k)}{f_k(i)} di. \quad (46)$$

In order to estimate the first integral in this expression, we recall that $f_{k+1}(I)$ increases, $R_{k+1}(I)$ decreases and $I_*^{k+1} \leq I_*^k$ due to Lemma 5, hence

$$\begin{aligned} 0 &\leq - \int_{I_*^k}^{I_*^{k+1}} \left(1 - \frac{f_{k+1}(I_*^{k+1})}{f_{k+1}(i)} \right) di \leq (I_*^k - I_*^{k+1}) \left(1 - \frac{f_{k+1}(I_*^{k+1})}{f_{k+1}(I_*^k)} \right) \\ &= (I_*^k - I_*^{k+1}) \frac{R_{k+1}(I_*^k)I_*^k - R_{k+1}(I_*^{k+1})I_*^{k+1}}{R_{k+1}(I_*^k)I_*^k} \leq (I_*^k - I_*^{k+1}) \frac{R_{k+1}(I_*^k)(I_*^k - I_*^{k+1})}{R_{k+1}(I_*^k)I_*^k} \\ &= \frac{(I_*^k - I_*^{k+1})^2}{I_*^k} \end{aligned} \quad (47)$$

and using Lemma 5 again,

$$- \int_{I_*^k}^{I_*^{k+1}} \left(1 - \frac{f_{k+1}(I_*^{k+1})}{f_{k+1}(i)} \right) di \leq \frac{\rho^2 q_0^2}{R_{k+1}^2(I_*^{k+1})R_k^2(I_*^k)I_*^k} (I_{k+1} - I_*^k)^2. \quad (48)$$

On the other hand,

$$\begin{aligned} &- \int_{I_*^k}^{I_*^{k+1}} \frac{f_{k+1}(I_*^{k+1}) - f_k(I_*^k)}{f_k(i)} di \\ &= - \int_{I_*^k}^{I_*^{k+1}} \frac{f_{k+1}(I_*^{k+1}) - f_{k+1}(I_*^k) + f_{k+1}(I_*^k) - f_k(I_*^k)}{f_k(i)} di \\ &= - \int_{I_*^k}^{I_*^{k+1}} \frac{I_*^{k+1}R_{k+1}(I_*^{k+1}) - I_*^kR_{k+1}(I_*^k) + I_*^k(R_{k+1}(I_*^k) - R_k(I_*^k))}{f_k(i)} di \\ &= \int_{I_*^k}^{I_*^{k+1}} \frac{I_*^{k+1}(R_{k+1}(I_*^k) - R_{k+1}(I_*^{k+1}))}{f_k(i)} di \\ &+ \int_{I_*^k}^{I_*^{k+1}} \frac{(I_*^k - I_*^{k+1})R_{k+1}(I_*^k) + I_*^k(R_k(I_*^k) - R_{k+1}(I_*^k))}{f_k(i)} di \\ &\leq \frac{I_{k+1} - I_*^k}{f_k(I_*^k)} ((I_*^k - I_*^{k+1})R_{k+1}(I_*^k) + I_*^k(R_k(I_*^k) - R_{k+1}(I_*^k))), \end{aligned} \quad (49)$$

where we used that $R_{k+1}(I_*^k) - R_{k+1}(I_*^{k+1}) \leq 0$ because $R_{k+1}(I)$ decreases and $f_k(I_*^k) \leq f_k(I)$ on $[I_*^k, I_{k+1}]$ because $f_k(I)$ increases. Hence, relations (40) and (41) imply

$$\begin{aligned} &- \int_{I_*^k}^{I_*^{k+1}} \frac{f_{k+1}(I_*^{k+1}) - f_k(I_*^k)}{f_k(i)} di \leq \frac{\rho q_0 R_{k+1}(I_*^k)(I_{k+1} - I_*^k)^2}{R_{k+1}(I_*^{k+1})R_k(I_*^k)f_k(I_*^k)} \\ &+ \frac{q_0 I_*^k (I_{k+1} - I_*^k)^2}{f_k(I_*^k)} \leq \frac{q_0 (I_{k+1} - I_*^k)^2}{R_k(I_*^k)} \left(\frac{\rho}{f_k(I_*^k)} + 1 \right). \end{aligned}$$

Combining this estimate with (46) and (48), we obtain (43). \square

Now we combine Lemmas 4 and 6 to obtain the following statement.

Lemma 7 *If $R_{r(t_k)}(I(t))S(t) > 1$ on (t_k, t_{k+1}) , then*

$$V_{k+1}(I_{k+1}, S_{k+1}) - V_k(I_k, S_k) \leq -Q_k(I_{k+1} - I_*^k)^2 \quad (50)$$

with

$$Q_k = \frac{\rho}{4} \sqrt{\frac{\epsilon_0 S_M}{2f_k(I_{k+1})}} - \frac{q_0}{R_k(I_*^k)} \left(\frac{\rho^2 q_0}{R_{k+1}^2(I_*^{k+1})f_k(I_*^k)} + \frac{\rho}{f_k(I_*^k)} + 1 \right), \quad (51)$$

where $M = (I_M, S_M)$ is the highest point of the level line $V_k(I, S) = V_k(I_{k+1}, S_{k+1})$ of the Lyapunov function V_k .

Proof. From Lemma 1, it follows that

$$\begin{aligned} \int_{I_*^k}^{I_{k+1}} \left(1 - \frac{f_k(I_*^k)}{f_k(i)} \right) di &= \int_{I_*^k}^{I_{k+1}} \frac{f_k(i) - f_k(I_*^k)}{f_k(i)} di \\ &\geq \int_{I_*^k}^{I_{k+1}} \frac{\epsilon_0(i - I_*^k)}{f_k(I_{k+1})} di \geq \frac{\epsilon_0(I_{k+1} - I_*^k)^2}{2f_k(I_{k+1})}. \end{aligned} \quad (52)$$

Substituting this estimate in (33) and adding (43), we obtain (50). \square

As the next step, we obtain a counterpart of Lemma 7 for the parts of the trajectory satisfying $R_{r(t_k)}(I(t))S(t) < 1$ on (t_k, t_{k+1}) .

Lemma 8 *If $R_{r(t_k)}(I(t))S(t) < 1$ on (t_k, t_{k+1}) , then*

$$V_{k+1}(I_{k+1}, S_{k+1}) - V_k(I_k, S_k) \leq -\tilde{Q}_k(I_{k+1} - I_*^k)^2 \quad (53)$$

with

$$\tilde{Q}_k = \frac{\rho}{4} \sqrt{\frac{\epsilon_0 S_m}{2f_k(I_*^k)}} - q_0 \left(\frac{\rho^2 q_0}{R_{k+1}^2(I_*^{k+1})R_k^2(I_*^k)I_*^k} + \frac{\rho R_{k+1}(I_*^k)}{R_{k+1}(I_*^{k+1})R_k(I_*^k)f_k(I_{k+1})} + \frac{I_*^k}{f_k(I_{k+1})} \right), \quad (54)$$

where $m = (I_m, S_m)$ is the lowest point of the level line $V_k(I, S) = V_k(I_{k+1}, S_{k+1})$ of the Lyapunov function V_k .

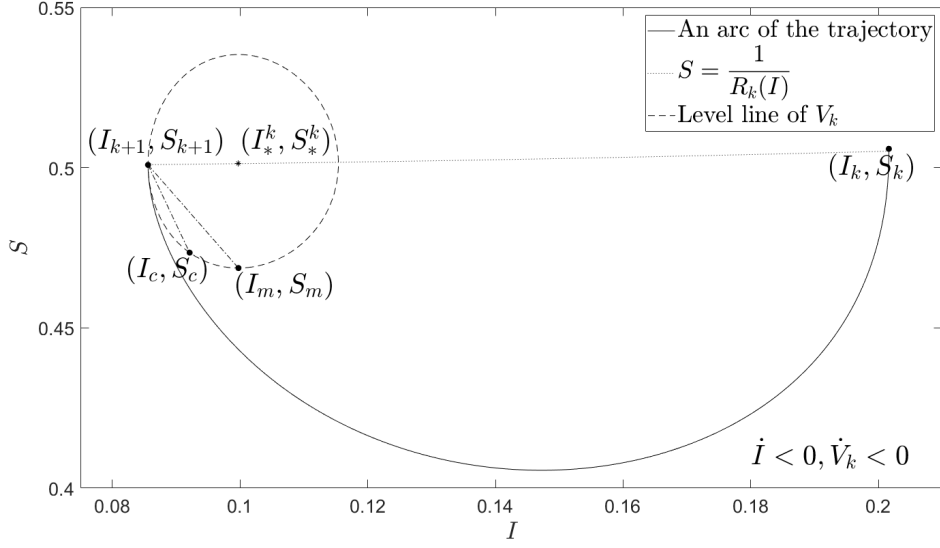


Figure 4: An arc of a trajectory of system (2), (13) satisfying $R_k(I(t))S(t) \leq 1$.

Proof. We adapt the proofs of Lemmas 4–6 to obtain their counterparts for the part of the trajectory satisfying $R_{r(t_k)}(I(t))S(t) < 1$ on (t_k, t_{k+1}) , which implies $\dot{I} < 0$. The main steps are outlined below for completeness.

The first coordinate of the point $m = (I_m, S_m)$ and the value of the Lyapunov function V_k at this point satisfy $I_m = I_*^k$ and

$$V_k(I_*^k, S_m) = S_m - S_*^k - S_*^k \ln \frac{S_m}{S_*^k} = V_k(I_{k+1}, S_{k+1}),$$

see Figure 4. Using Lemma 3, we obtain the estimate

$$I_*^k - I_c \geq I_*^k - I_{k+1} - \frac{S_{k+1} - S_c}{S_{k+1} - S_m} (I_*^k - I_{k+1}) = \frac{S_c - S_m}{S_{k+1} - S_m} (I_*^k - I_{k+1}) \quad (55)$$

for any point (I_c, S_c) that belongs to the arc of the level line of V_k connecting the points m and $(I_{k+1}, S_{k+1}) = (I_{k+1}, 1/R_k(I_{k+1}))$ (cf. (34)).

Using (30) in the domain $I \leq I_*^k$, $S \leq 1/R_k(I)$, we obtain that along the trajectory

$$\frac{dV_k}{dI} \geq -\frac{\rho(S - S_*^k)^2}{SS_*^k(R_k(I)S - 1)I} \geq 0,$$

where $1/R_k(I) \leq 1/R_k(I_*^k) = S_*^k$ implies $0 \leq 1/R_k(I) - S \leq S_*^k - S$, hence

$$\frac{dV_k}{dI} \geq \frac{\rho(S - S_*^k)^2}{SS_*^k R_k(I)I(S_*^k - S)} = \frac{\rho}{SS_*^k R_k(I)I} (S_*^k - S)$$

and due to $R_k(I)S < 1$, $S_*^k \leq 1$,

$$\frac{dV_k}{dI} \geq \frac{\rho(S_*^k - S)}{I}.$$

Since the trajectory lies below the level line of V_k , on the interval $[I_c, I_*]$ we have $S \leq S_c$ and $\frac{dV_k}{dI} \geq \frac{\rho}{I}(S_*^k - S_c)$, which implies

$$V_k(I_*^k, \hat{S}(I_*^k)) - V_k(I_c, \hat{S}(I_c)) \geq \rho(S_*^k - S_c) \ln \frac{I_*^k}{I_c},$$

where $(I, \hat{S}(I))$, $I \in [I_{k+1}, I_k]$ is a parameterization of the segment of the trajectory, and using the identity $\ln(1+x) \geq x/(1+x)$, $x \geq -1$, we obtain

$$\begin{aligned} V_k(I_c, \hat{S}(I_c)) - V_k(I_*^k, \hat{S}(I_*^k)) &\leq -\rho(S_*^k - S_c) \frac{I_*^k - I_c}{I_*^k} \\ &\leq -\rho \frac{(S_*^k - S_c)(S_c - S_m)(I_*^k - I_{k+1})}{S_{k+1} - S_m}, \end{aligned}$$

where in the last step we used $I_*^k \leq 1$ and (55). Maximizing the right hand side of this formula over $S_c \in [S_m, S_{k+1}]$ as in the proof of Lemma 4 and taking into account that the function V_k decreases along the trajectory, we arrive at (cf. (37))

$$\Delta V_k = V_k(I_{k+1}, S_{k+1}) - V_k(I_k, S_k) \leq -\frac{\rho}{4}(S_*^k - S_m)(I_*^k - I_{k+1}). \quad (56)$$

In order to estimate the difference $S_*^k - S_m$ in (56), we equate the values of the function V_k at the points (I_*^k, S_m) and (I_{k+1}, S_{k+1}) to obtain

$$S_*^k \ln \frac{S_{k+1}}{S_m} - (S_{k+1} - S_m) = \int_{I_{k+1}}^{I_*^k} \left(\frac{f_k(I_*^k)}{f_k(i)} - 1 \right) di.$$

Using the inequality $2(1+x) \ln(1+x) \leq x(2+x)$, $x \geq 0$ we get

$$\ln \frac{S_{k+1}}{S_m} \leq \frac{S_{k+1}^2 - S_m^2}{2S_{k+1}S_m},$$

where $S_m < S_{k+1} < S_*^k$, therefore

$$\begin{aligned} S_*^k \ln \frac{S_{k+1}}{S_m} - (S_{k+1} - S_m) &\leq (S_{k+1} - S_m) \left(\frac{S_*^k(S_{k+1} + S_m)}{2S_{k+1}S_m} - 1 \right) \\ &= \frac{S_{k+1} - S_m}{2} \left(\frac{S_*^k - S_m}{S_m} + \frac{S_*^k - S_{k+1}}{S_{k+1}} \right) \leq \frac{(S_*^k - S_m)^2}{S_m}, \end{aligned}$$

hence

$$\frac{(S_*^k - S_m)^2}{S_m} \geq \int_{I_{k+1}}^{I_*^k} \left(\frac{f_k(I_*^k)}{f_k(i)} - 1 \right) di$$

and from (56) it follows that (cf. (33))

$$\Delta V_k \leq -\frac{\rho}{4}(I_*^k - I_{k+1}) \sqrt{S_m \int_{I_{k+1}}^{I_*^k} \left(\frac{f_k(I_*^k)}{f_k(i)} - 1 \right) di}.$$

Further, due to Lemma 1,

$$\int_{I_*^k}^{I_{k+1}} \left(1 - \frac{f_k(I_*^k)}{f_k(i)} \right) di \geq \frac{\epsilon_0(I_{k+1} - I_*^k)^2}{2f_k(I_*^k)},$$

consequently,

$$\Delta V_k \leq -\frac{\rho}{4}(I_*^k - I_{k+1})^2 \sqrt{\frac{\epsilon_0 S_m}{2f_k(I_*^k)}}. \quad (57)$$

As in the proof of Lemma 5,

$$S_*^k - S_*^{k+1} = \frac{I_*^{k+1} - I_*^k}{\rho} = \frac{1}{R_k(I_*^k)R_{k+1}(I_*^{k+1})} (R'_{k+1}(\hat{I})(I_*^{k+1} - I_*^k) + R_{k+1}(I_*^k) - R_k(I_*^k))$$

but this time (cf. (41))

$$0 \leq R_k(I_*^{k+1}) - R_k(I_*^k) \leq q_0(I_*^k - I_{k+1}), \quad (58)$$

which allows us to conclude (due to $R'_{k+1}(\hat{I}) \leq 0$) that $I_*^{k+1} \geq I_*^k$ and $S_*^{k+1} \leq S_*^k$, and the argument used in the proof of Lemma 5 leads to the estimates (cf. (40))

$$0 \leq I_*^{k+1} - I_*^k = \rho(S_*^k - S_*^{k+1}) \leq \frac{\rho q_0}{R_{k+1}(I_*^{k+1})R_k(I_*^k)} (I_*^k - I_{k+1}). \quad (59)$$

In particular, as opposed to the case considered in Lemmas 4–6,

$$I_*^{k+1} \geq I_*^k \geq I_{k+1}, \quad S_{k+1} \leq S_*^{k+1} \leq S_*^k, \quad (60)$$

while

$$R_k(I) \leq R_{k+1}(I) \quad \text{for } I \geq I_{k+1}. \quad (61)$$

Using the notation Δ_S and Δ_I introduced in the proof of Lemma 6, from (60) we obtain (44) and $\Delta_S \leq 0$, while (61) leads to (45), hence the difference (39) satisfies

(46). Further, relation (47) also holds true, hence (59) implies (48). Finally, a counterpart of (49) reads

$$\begin{aligned} & - \int_{I_*^k}^{I_{k+1}} \frac{f_{k+1}(I_*^{k+1}) - f_k(I_*^k)}{f_k(i)} di \\ & \leq \frac{I_*^k - I_{k+1}}{f_k(I_{k+1})} ((I_*^{k+1} - I_*^k)R_{k+1}(I_*^k) + I_*^k(R_{k+1}(I_*^k) - R_k(I_*^k))) \end{aligned}$$

and due to (58) and (59),

$$- \int_{I_*^k}^{I_{k+1}} \frac{f_{k+1}(I_*^{k+1}) - f_k(I_*^k)}{f_k(i)} di \leq \frac{q_0(I_*^k - I_{k+1})^2}{f_k(I_{k+1})} \left(\frac{\rho R_{k+1}(I_*^k)}{R_{k+1}(I_*^{k+1})R_k(I_*^k)} + I_*^k \right).$$

Combining this estimate with (46) and (48), we obtain (cf. (43))

$$\tilde{\Delta}V_k \leq q_0(I_*^k - I_{k+1})^2 \left(\frac{\rho^2 q_0}{R_{k+1}^2(I_*^{k+1})R_k^2(I_*^k)I_*^k} + \frac{\rho R_{k+1}(I_*^k)}{R_{k+1}(I_*^{k+1})R_k(I_*^k)f_k(I_{k+1})} + \frac{I_*^k}{f_k(I_{k+1})} \right)$$

and adding (57) leads to (53). \square

In order to use Lemmas 7 and 8 we need to estimate the components $I(t), S(t)$ of the trajectory from below.

Lemma 9 For $t \geq t_2$,

$$I(t) \geq i_0 := \rho \frac{R_0^{int} - 1}{R_0^{int}} e^{-\left(\frac{2}{\rho(R_0^{int}-1)} + \frac{1}{R_0^{int}}\right)R_0^{nat}}, \quad S(t) \geq s_0 := \frac{e^{-(1+2R_0^{nat})}}{R_0^{nat}}. \quad (62)$$

Proof. Consider a point $(I_k, S_k) = (I_k, 1/R_k(I_k))$ where the trajectory satisfies $\dot{I} = 0, \dot{S} < 0$, see Figure 4. At this point,

$$V_k(I_k, S_k) = \int_{I_*^k}^{I_k} \left(1 - \frac{f_k(I_*^k)}{f_k(i)}\right) di + \int_{S_*^k}^{S_k} \left(1 - \frac{S_*^k}{s}\right) ds \leq S_k - S_*^k + I_k - I_*^k \leq 2.$$

Clearly, the minimal value $s_m^k = \min_{t \in [t_k, t_{k+2}]} S(t)$ of the S -component of the trajectory over the time interval $[t_k, t_{k+2}]$ is achieved at a time $t_m^k \in [t_k, t_{k+1}]$, i.e. $s_m^k = S(t_m^k)$. Since V_k decreases on the time interval $[t_k, t_{k+1}]$, from $V_k(I_k, S_k) \leq 2$, it follows that

$$2 \geq V_k(I(t_m^k), S(t_m^k)) \geq \int_{s_m^k}^{S_*^k} \left(\frac{S_*^k}{s} - 1\right) ds = S_*^k \ln \frac{S_*^k}{s_m^k} - (S_*^k - s_m^k) \geq S_*^k \ln \frac{S_*^k}{s_m^k} - S_*^k.$$

Therefore, $s_m^k \geq S_*^k e^{-\left(1+\frac{2}{S_*^k}\right)}$ and due to $S_*^k \geq 1/R_0^{nat}$,

$$s_m^k = \min_{t \in [t_k, t_{k+2}]} S(t) \geq \frac{e^{-(1+2R_0^{nat})}}{R_0^{nat}}.$$

On the other hand, the minimal value $i_m^k = \min_{t \in [t_k, t_{k+2}]} I(t)$ of the I -component of the trajectory over the time interval $[t_k, t_{k+2}]$ is achieved at the point (I_{k+1}, S_{k+1}) , i.e. $i_m^k = I_{k+1}$. Again, since V_k decreases on the time interval $[t_k, t_{k+1}]$, from $V_k(I_k, S_k) \leq 2$, it follows that

$$\begin{aligned} 2 \geq V_k(I_{k+1}, S_{k+1}) &\geq \int_{I_{k+1}}^{I_*^k} \left(\frac{f_k(I_*^k)}{f_k(i)} - 1 \right) di = f_k(I_*^k) \int_{I_{k+1}}^{I_*^k} \frac{di}{i R_k(i)} - (I_*^k - I_{k+1}) \\ &\geq \frac{f_k(I_*^k)}{R_0^{nat}} \int_{I_{k+1}}^{I_*^k} \frac{di}{i} - I_*^k = \frac{f_k(I_*^k)}{R_0^{nat}} \ln \frac{I_*^k}{I_{k+1}} - I_*^k, \end{aligned}$$

hence

$$I_{k+1} \geq I_*^k e^{-(2+I_*^k) \frac{R_0^{nat}}{f_k(I_*^k)}} = I_*^k e^{-\left(\frac{2}{I_*^k R_k(I_*^k)} + \frac{1}{R_k(I_*^k)}\right) R_0^{nat}}.$$

Therefore, using $I_*^k = \rho(1 - S_*^k)$ and $S_*^k = 1/R_k(I_*^k) \leq 1/R_0^{int}$, we obtain

$$I_{k+1} = \min_{t \in [t_k, t_{k+2}]} I(t) \geq \rho(1 - S_*^k) e^{-\left(\frac{2}{\rho(1-S_*^k)} + 1\right) S_*^k R_0^{nat}} \geq \rho \frac{R_0^{int} - 1}{R_0^{int}} e^{-\left(\frac{2}{\rho(R_0^{int}-1)} + \frac{1}{R_0^{int}}\right) R_0^{nat}},$$

which completes the proof. \square

We can now prove the convergence of the trajectories to the equilibrium set.

Lemma 10 *Every trajectory of system (2), (13) with initial values $I(0) > 0, S(0) > 0$ converges to the set of endemic equilibrium states.*

Proof. From Lemmas 7–9, it follows that the sequence $v_k = V_k(I_k, S_k)$ satisfies

$$v_{k+1} - v_k \leq -\kappa(I_*^k - I_{k+1})^2, \quad k = 0, 1, 2, \dots \quad (63)$$

with

$$\kappa := \frac{\rho}{4} \sqrt{\frac{\epsilon_0 s_0}{2R_0^{nat}}} - \frac{q_0}{i_0 R_0^{int}} \left(\frac{\rho^2 q_0}{(R_0^{int})^3} + \frac{\rho R_0^{nat}}{(R_0^{int})^2} + 1 \right) > 0, \quad (64)$$

independent of k .

Since $f(I) = R(I)I \leq R_0^{nat}$ for $0 \leq I \leq 1$, Lemma 1 implies that

$$\int_{I_*^k}^I \frac{f_k(i) - f_k(I_*^k)}{f_k(i)} di \geq \frac{\epsilon_0}{R_0^{nat}} \int_{I_*^k}^I (i - I_*^k) di = \frac{\epsilon_0}{2R_0^{nat}} (I - I_*^k)^2.$$

On the other hand,

$$f'_k(I) = (IR_k(I))' = R'_k(I)I + R_k(I) \leq R_k(I) \leq R_0^{nat}, \quad f_k(I) = IR_k(I) \geq i_0 R_0^{int},$$

where i_0 is defined in (62), hence

$$\int_{I_*^k}^I \frac{f_k(i) - f_k(I_*^k)}{f_k(i)} di \leq \frac{R_0^{nat}}{i_0 R_0^{int}} \int_{I_*^k}^I (i - I_*^k) di = \frac{R_0^{nat}}{2i_0 R_0^{int}} (I - I_*^k)^2,$$

so we have

$$\frac{\epsilon_0}{2R_0^{nat}} (I - I_*^k)^2 \leq \int_{I_*^k}^I \frac{f_k(i) - f_k(I_*^k)}{f_k(i)} di \leq \frac{R_0^{nat}}{2i_0 R_0^{int}} (I - I_*^k)^2. \quad (65)$$

Similarly, due to $0 \leq S \leq 1$,

$$\frac{(S - S_*^k)^2}{2} \leq \int_{S_*^k}^S \left(1 - \frac{S_*^k}{s}\right) ds \leq \frac{(S - S_*^k)^2}{2s_0}, \quad (66)$$

with s_0 defined in (62). Adding (65) and (66), we obtain

$$\frac{\epsilon_0 (I - I_*^k)^2}{2R_0^{nat}} + \frac{(S - S_*^k)^2}{2} \leq V_k(I, S) \leq \frac{R_0^{nat} (I - I_*^k)^2}{2i_0 R_0^{int}} + \frac{(S - S_*^k)^2}{2s_0}. \quad (67)$$

Relation (63) implies

$$v_n = v_1 + \sum_{k=1}^{n-1} (v_{k+1} - v_k) \leq v_1 - \kappa \sum_{k=1}^{n-1} (I_*^k - I_{k+1})^2,$$

and due to the non-negativity of each Lyapunov function V_n ,

$$\sum_{k=1}^{n-1} (I_*^k - I_{k+1})^2 \leq \frac{1}{\kappa} v_1$$

for any n , hence

$$\sum_{k=1}^{\infty} (I_*^k - I_{k+1})^2 < \infty.$$

Therefore $I_{k+1} - I_*^k \rightarrow 0$ (as $k \rightarrow \infty$). Due to (4) and (59), this implies $I_k - I_*^k \rightarrow 0$, and from $S_*^k = 1/R_k(I_*^k)$, $S_k = 1/R_k(I_k)$ it follows that $S_k - S_*^k \rightarrow 0$. Hence, (67) implies $v_k = V_k(I_k, S_k) \rightarrow 0$. Since V_k is nonnegative and decreases along the trajectory, we conclude that

$$V_k(I_k, S_k) = \max_{t \in [t_k, t_{k+1}]} V_k(I(t), S(t)) \rightarrow 0 \quad \text{as } k \rightarrow \infty, \quad (68)$$

hence (67) implies that the trajectory converges to the equilibrium set. \square

It remains to show that every trajectory converges to an equilibrium. The following lemma completes the proof of the theorem.

Lemma 11 *Every trajectory of system (2), (13) with positive initial values $I(0), S(0)$ converges to an endemic equilibrium state.*

Proof. From (67), it follows that

$$V_k(I_{k+1}, S_{k+1}) \leq \frac{R_0^{nat}}{2i_0 R_0^{int}} (I_{k+1} - I_*^k)^2 + \frac{1}{2s_0} \left(\frac{1}{R_k(I_{k+1})} - \frac{1}{R_k(I_*^k)} \right)^2,$$

where $R_k(I) \geq R_0^{int}$ and $|R_k(I_{k+1}) - R_k(I_*^k)| \leq q_0 |I_{k+1} - I_*^k|$ due to (22), hence

$$V_k(I_{k+1}, S_{k+1}) \leq a(I_{k+1} - I_*^k)^2, \quad a := \frac{R_0^{nat}}{2i_0 R_0^{int}} + \frac{q_0}{2s_0 (R_0^{int})^2}. \quad (69)$$

Lemma 6 implies that

$$\tilde{\Delta} V_k \leq b(I_{k+1} - I_*^k)^2, \quad b := \frac{q_0}{R_0^{int}} \left(\frac{\rho^2 q_0}{i_0 R_0^{int} (R_0^{int})^2} + \frac{\rho}{i_0 R_0^{int}} + 1 \right),$$

hence, using (69),

$$V_{k+1}(I_{k+1}, S_{k+1}) = V_k(I_{k+1}, S_{k+1}) + \tilde{\Delta} V_k \leq (a + b)(I_{k+1} - I_*^k)^2. \quad (70)$$

If $V_k(I_k, S_k) \geq (a + b + \kappa)(I_{k+1} - I_*^k)^2$ with κ defined by (64), then (70) implies

$$v_{k+1} = V_{k+1}(I_{k+1}, S_{k+1}) \leq p V_k(I_k, S_k) = p v_k, \quad p := \frac{a + b}{a + b + \kappa} < 1. \quad (71)$$

On the other hand, if $V_k(I_k, S_k) \leq (a + b + \kappa)(I_{k+1} - I_*^k)^2$, then (63) implies (71). Therefore, in either case,

$$v_k \leq v_0 p^k. \quad (72)$$

Since V_k decreases along the trajectory, $V_k(I_{k+1}, S_{k+1}) \leq V_k(I_k, S_k) = v_k$. But according to (67),

$$V_k(I_{k+1}, S_{k+1}) \geq \frac{\epsilon_0}{2R_0^{nat}} (I_{k+1} - I_*^k)^2, \quad (73)$$

hence

$$\frac{\epsilon_0}{2R_0^{nat}} (I_{k+1} - I_*^k)^2 \leq v_k \leq v_0 p^k.$$

Further, according to (40), (59),

$$|I_*^{k+1} - I_*^k| \leq \frac{\rho q_0}{(R_0^{int})^2} |I_{k+1} - I_*^k|,$$

consequently

$$|I_*^{k+1} - I_*^k| \leq \frac{\rho q_0}{(R_0^{int})^2} \sqrt{\frac{2v_0 R_0^{nat}}{\epsilon_0}} p^{\frac{k}{2}}.$$

We see that I_*^k is a Cauchy sequence, hence it converges to a limit value I_* . Since $I_{k+1} - I_*^k \rightarrow 0$ as $k \rightarrow \infty$, we conclude that $I(t) \rightarrow I_*$ as $t \rightarrow \infty$, which implies that each of the functions $R_0(t)$ and $S(t)$ also has a limit as $t \rightarrow \infty$. Denoting the limit of $S(t)$ by S_* , the trajectory converges to the equilibrium (I_*, S_*) . \square

References

- [1] Balanov Z, Krawcewicz W, Rachinskii D, Zhezherun A (2012) Hopf bifurcation in symmetric networks of coupled oscillators with hysteresis. *Journal of Dynamics and differential Equations* 24(4):713-759
- [2] Brokate M, Pokrovskii A, Rachinskii D (2006) Asymptotic stability of continuum sets of periodic solutions to systems with hysteresis. *Journal of Mathematical Analysis and Applications* 319(1):94-109
- [3] Brokate M, Sprekels J (1996) *Hysteresis and phase transitions*. Springer, New York
- [4] Capasso V, Serio G (1978) A generalization of the Kermack-Mckendrick deterministic epidemic model. *Math Biosci* 42:43-61. [https://doi.org/10.1016/0025-5564\(78\)90006-8](https://doi.org/10.1016/0025-5564(78)90006-8)
- [5] Center of Disease Control and Prevention (CDC), USA (2021) Implementation of mitigation strategies for communities with local COVID-19 transmission. <https://www.cdc.gov/coronavirus/2019-ncov/community/community-mitigation.html>
- [6] Chen FH (2004) Rational behavioral response and the transmission of STDs. *Theor Popul Biol* 66:307-316. doi: 10.1016/j.tpb.2004.07.004
- [7] Chen X, Fu F(2019) Imperfect vaccine and hysteresis. *Proc R Soc B* 286(1894):20182406. <http://doi.org/10.1098/rspb.2018.2406>
- [8] Chernorutskii V, Rachinskii D (1997) On uniqueness of an initial-value problem for ODE with hysteresis. *Nonlinear Differential Equations and Applications NoDEA* 4 (3), 391-399
- [9] Chladná Z, Kopfová J, Rachinskii D, Rouf SC (2020) Global dynamics of SIR model with switched transmission rate. *J Math Biol* 80:1209-1233.
- [10] Debenedetto P, Ruiz B (2021) Houston region passes threshold for tougher COVID-19 restrictions. Houston Public Media. <https://www.houstonpublicmedia.org/articles/news/health-science/coronavirus/2021/01/05/388740/houston-area-projected-to-pass-governors-threshold-for-tougher-covid-19-restrictions-hidalgo-says/>
- [11] Department of Health and Human Services, Nebraska (2020) Phased public health restrictions tied to coronavirus hospitalization rate. <https://dhhs.ne.gov/Documents/DHM-Measure-Table-ENGLISH.pdf>

- [12] Di Bernardo M, Crowther-Swanepoel D, Broderick P et al (2008) A genome-wide association study identifies six susceptibility loci for chronic lymphocytic leukemia. *Nat Genet* 40:1204–1210. doi: 10.1038/ng.219
- [13] d’Onofrio A, Manfredi P (2009) Information-related changes in contact patterns may trigger oscillations in the endemic prevalence of infectious diseases. *J Theor Biol* 256:473-478. doi: 10.1016/j.jtbi.2008.10.005
- [14] d’Onofrio A, Manfredi P (2020) The interplay between voluntary vaccination and reduction of risky behavior: A general behavior-implicit SIR model for vaccine preventable infections. In: Maira Aguiar et al (eds) *Current Trends in Dynamical Systems in Biology and Natural Sciences*. Springer, Switzerland, pp 185-203. doi:10.1007/978-3-030-41120-6_10
- [15] Ewing JA (1885). Experimental research in magnetism. *Philos Trans R Soc Lond* 176: 523-640
- [16] Fairlie R (2020) The impact of COVID-19 on small business owners: Evidence from the first three months after widespread social distancing restrictions. *J Econ Manag Strategy* 29:727-740. doi: 10.1111/jems.12400
- [17] Fathian K, Rachinskii DI, Spong MW, Summers TH, Gans NR (2019) Distributed formation control via mixed barycentric coordinate and distance-based approach. *American Control Conference (ACC)* 51-58
- [18] Friedman G, McCarthy S, Rachinskii D (2014) Hysteresis can grant fitness in stochastically varying environment. *PLOS ONE* 9(7):e103241
- [19] Geoffard PY, Philipson T (1996) Rational epidemics and their public control. *Int Econ Rev* 37:603-624. doi.org/10.2307/2527443
- [20] Gostin LO, Wiley LF (2020) Governmental public health powers during the COVID-19 pandemic: Stay-at-home orders, business closures, and travel restrictions. *JAMA* 323:2137-2138. doi: 10.1001/jama.2020.5460
- [21] Guidry JPD, Laestadius LI, Vraga EK, Miller CA, Perrin PB, Burton CW, Ryan M, Fuemmeler BF, Carlyle KE (2021) Willingness to get the COVID-19 vaccine with and without emergency use authorization. *Am J Infect Control* 49:137-142. doi: 10.1016/j.ajic.2020.11.018
- [22] Haderler KP, Castillo-Chavez C (1995) A core group model for disease transmission. *Math Biosci* 128:41-55. doi: 10.1016/0025-5564(94)00066-9

- [23] Hooton E, Balanov Z, Krawcewicz W, Rachinskii D (2017) Noninvasive stabilization of periodic orbits in symmetrically coupled systems near a Hopf bifurcation point. *International Journal of Bifurcation and Chaos* 27(06):1750087
- [24] Hazewinkel M (1997) *Kluwer encyclopedia of mathematics: Supplement 1*. Kluwer Acad Publ, pp 310-384
- [25] Hoppensteadt FC, Jäger W (1980) Pattern formation by bacteria. In: Jäger W, Rost H, Tautu P (eds) *Biological growth and spread: Lecture notes in biomathematics*, vol 38. Springer, Berlin, pp 68-81
- [26] Kermack WO, McKendrick AG (1927) A contribution to the mathematical theory of epidemics. *Proc R Soc Lond A* 115:700–721. doi: 10.1098/rspa.1927.0118
- [27] Kopfová J, Nábelková P, Rachinskii D, Rouf SC (2021) Dynamics of SIR model with vaccination and heterogeneous behavioral response of individuals modeled by the Preisach operator. *J Math Biology*, 83, 11. doi: 10.1007/s00285-021-01629-8
- [28] Krasnosel'skii MA, Pokrovskii AV (1989) *Systems with Hysteresis*. Springer, Berlin, Heidelberg
- [29] Krasnosel'skii A, Rachinskii D (2002) On a bifurcation governed by hysteresis nonlinearity. *Nonlinear Differential Equations and Applications NoDEA*, 9(1):93-115
- [30] Krasnosel'skii AM, Rachinskii DI (2002) On the existence of cycles in autonomous systems. *Doklady Mathematics* 65(3):344-349
- [31] Krejčí P (1996) *Hysteresis, convexity and dissipation in hyperbolic equations*. Gakkotosho, Tokyo
- [32] Krejčí P, Kaltenbacher B (2019) Analysis of optimization problem for a piezoelectric energy harvester. *Arch Appl Mech* 89:1103-1122
- [33] Lazarus JV, Ratzan SC, Palayew A et al (2021) A global survey of potential acceptance of a COVID-19 vaccine. *Nat Med* 27:225. doi: 10.1038/s41591-020-1124-9
- [34] Leonov G, Shumafov M, Teshev V, Aleksandrov K (2017) Differential equations with hysteresis operators: Existence of solutions, stability, and oscillations. *Differ Equ* 53:1764-1816.

- [35] Marquioni VM, De Aguiar M (2020) Quantifying the effects of quarantine using an IBM SEIR model on scalefree networks. *Chaos Solitons Fractals* 138:109999. doi:10.1016/j.chaos.2020.109999
- [36] Matrajt L, Leung T (2020) Evaluating the effectiveness of social distancing interventions to delay or flatten the epidemic curve of coronavirus disease. *Emerg Infect Dis* 26:1740-1748. doi: 10.3201/eid2608.201093
- [37] Mayergoyz ID (2003) *Mathematical models of hysteresis and their applications*. Academic Press, New York
- [38] Pimenov A, Kelly TC, Korobeinikov A, O’Callaghan MJA, Pokrovskii A, Rachinskii D (2012) Memory effects in population dynamics: Spread of infectious disease as a case study. *Math Model Nat Phenom* 7:1-30
- [39] Rachinskii D (2015) Realization of arbitrary hysteresis by a low-dimensional gradient flow. *Discrete and Continuous Dynamical Systems B* 21(1):227-243. Arxiv preprint arXiv:1506.03842
- [40] Rachinskii D, Ruderman M (2016) Convergence of direct recursive algorithm for identification of Preisach hysteresis model with stochastic input. *SIAM Journal on Applied Mathematics* 76(4):1270-1295
- [41] Reluga TC, Bauch CT, Galvani AP (2006) Evolving public perceptions and stability in vaccine uptake. *Math Biosci* 204:185-98. doi: 10.1016/j.mbs.2006.08.015
- [42] Rouf S, Rachinskii D (2021) Dynamics of SIR model with heterogeneous response to intervention policy. arXiv:2103.07989
- [43] Su Z, Wang W, Li L, Xiao J, Stanley HE (2017) Emergence of hysteresis loop in social contagions on complex networks. *Sci Rep* 7, 6103. <https://doi.org/10.1038/s41598-017-06286-w>
- [44] Visintin A (1994) *Hysteresis and semigroups: In differential models of hysteresis*. Springer, Berlin, Heidelberg, pp 211-256
- [45] Wang W, Tang M, Stanley HE, Braunstein LA (2017) Unification of theoretical approaches for epidemic spreading on complex networks. *Rep Prog Phys* 80:036603. <https://doi.org/10.1088/1361-6633/aa5398>
- [46] Wilder-Smith A, Chiew CJ, Lee VJ (2020) Can we contain the COVID-19 outbreak with the same measures as for SARS? *Lancet Infect Dis* 20:102-107. doi: 10.1016/S1473-3099(20)30129-8

- [47] Yakubovich VA, Leonov GA, Gelig AK (2004) Stability of stationary sets in control systems with discontinuous nonlinearities. World Scientific, Singapore